University of Nevada, Reno

Antibody interactions with the capsular polysaccharide of *Burkholderia pseudomallei*

A dissertation submitted in partial fulfillment of the requirements for the degree of

Doctor of Philosophy in Cell and Molecular Biology

By: Michael J. Dillon

Dr. David P. AuCoin/Dissertation Advisor

December 2014

THE GRADUATE SCHOOL

University of Nevada, Reno
Statewide · Worldwide

We recommend that the dissertation
prepared under our supervision by

Michael James Dillon

entitled

Antibody interactions with the capsular polysaccharide of *Burkholderia pseudomallei*

be accepted in partial fulfillment of the
requirements for the degree of

DOCTOR OF PHILOSOPHY

David P. AuCoin, Ph.D., Advisor

Thomas R. Kozel, Ph.D., Committee Member

Gregory S. Pari, Ph.D., Committee Member

Subhash C. Verma Ph.D., Committee Member

Kathleen M. Schegg Ph.D., Graduate School Representative

David W. Zeh, Ph.D., Dean, Graduate School

December, 2014

Abstract

Burkholderia pseudomallei is an important human pathogen that causes melioidosis. Infection is highly lethal and notoriously difficult to diagnose and treat. As such, it has tremendous bioterror potential and has been classified as a Tier 1 select agent by the Centers for Disease Control and the Department of Health & Human Services. One reason that *B. pseudomallei* is a successful pathogen is that it is surrounded by a high molecular weight capsular polysaccharide (CPS) comprised of *manno*heptopyranose residues. CPS inhibits complement deposition, prevents phagocytosis, and greatly enhances virulence. Previous studies have indicated that antibodies targeting CPS have high therapeutic value and can be used to diagnose *B. pseudomallei* infection.

The present work describes the development and characterization of 15 monoclonal antibodies (mAbs) in an effort to further the understanding of how antibodies interact with *B. pseudomallei* CPS. We have generated two complete Immunoglobulin G (IgG) subclass families; subclass families are antibodies that have identical variable regions, but different constant regions, and thus different effector functions. We have determined that some of these mAbs are protective in a murine model of pulmonary melioidosis in a subclass-independent manner. In this study, protection appears to be a function of mAb binding affinity. Additionally, we determined that non-IgG$_3$ mAbs are best for diagnosing active infection. Isolating a high affinity IgG$_3$ and generating a subclass-switch family yielded mAbs with low affinities that did not perform well in a diagnostic test

format. Thus, immunization strategies should focus on eliciting alternative IgG immune responses. Using this information, we have updated a prototype Active Melioidosis Detect™ Lateral Flow Immunoassay (AMD LFI) by replacing the original IgG_3 mAb with a high affinity IgG_1 mAb. This updated AMD LFI has increased sensitivity, is highly specific, and rapid; it can detect *B. pseudomallei* CPS in multiple sample types in 15 minutes or less.

<u>Dedication</u>

For my trusty pups Jackson & Houston. I couldn't wish for better friends. ☺

<u>Acknowledgements</u>

I would like to express my heartfelt gratitude to Dr. David AuCoin for the opportunity to pursue my doctoral studies in his laboratory. I will always be grateful for this experience and I will never forget the lessons I have learned under your guidance.

Additionally, I must thank each and every member in our laboratory, students and staff alike. I greatly appreciate all of the assistance learning new techniques and concepts, all of the countless hours reviewing papers and posters, and all of the many years preparing me to become a scientist. I could never have done it without the help and support you have all so graciously provided me.

I would also like to acknowledge my committee members: Dr. Thomas Kozel, Dr. Gregory Pari, Dr. Subash Verma, and Dr. Kathleen Schegg. Thank you all for bestowing upon me your infinite wealth of knowledge and expertise.

Table of Contents   **Page #**

Figures & Tables   **Page #**

Introduction

This work describes the development of a library of monoclonal antibodies (mAbs) to diagnose and/or treat *Burkholderia pseudomallei* infection. A brief introduction on each component of the research will be given, including pertinent information on *B. pseudomallei* and the disease it causes, melioidosis. Additionally, brief introductions on bacterial capsules, antibodies, and immunity will be given. Finally, laboratory diagnostic methods that incorporate antibodies will be covered, with an emphasis on lateral flow immunoassays.

Endemicity and epidemiology of *Burkholderia pseudomallei*

B. pseudomallei is a soil-dwelling, gram-negative bacillus endemic to Southeast Asia and Northern Australia. It thrives in aqueous environments and its geographical distribution ranges from roughly 20 degrees north and south of the equator (1). This region is expanding as global climate conditions allow for more favorable *B. pseudomallei* replication; temperatures are staying warmer farther from the equator and monsoons are pushing farther inland (1). The bacterium is ubiquitous in endemic regions; it is so common that, by the age of 4, 80% of all Thai children have circulating antibodies against *B. pseudomallei* antigens (2).

B. pseudomallei readily infects through contact with dermal abrasions, ingestion, or inhalation (3). It is an opportunistic pathogen and will not usually cause serious disease in healthy individuals. Predisposing factors are conditions that impair neutrophil function, including diabetes mellitus, thalassaemia, renal disease, and alcohol abuse; 50% of all melioidosis patients are diabetic (4).

Patients with diabetes exhibit reduced neutrophil migration to sites of infection due to impaired regulation of TNF-α (5). In general, innate immunity mechanisms do not seem to contribute to patient survival. Instead, survival rates are correlated with high antibody titers to *B. pseudomallei* antigens (1).

Diagnosis and treatment of *B. pseudomallei* infection

B. pseudomallei is the causative agent of melioidosis and infects roughly 21 out of every 100,000 people in Northeast Thailand. Infection is highly lethal, causing fatal sepsis in almost 50% of all patients in Thailand (6). Of the survivors, 25% will relapse, which it thought to be caused from reactivation of latent *B. pseudomallei* reservoirs in internal organs. Melioidosis is the third most common cause of death from infectious disease in Northeast Thailand, behind human immunodeficiency virus (HIV) and tuberculosis. Even in Australia, where access to intensive therapy is more readily available, mortality rates are still as high 20% (6). Globally, there are an estimated 250,000 deaths each year attributed to melioidosis (personal communication Dr. Direk Limmathurotsakul).

B. pseudomallei infection is notoriously difficult to diagnose and treat. Melioidosis presents as a febrile illness and mimics the symptoms of many other diseases including tuberculosis and other influenza-like illness. The vast majority of patients present with pneumonia and/or bacteremia (7). Severity ranges from rapid onset septicemia to chronic infection. Patients usually experience a 7-10 day incubation period before the onset of symptoms, however, there have been reported cases of latent infections taking several years to manifest (8, 9).

Culturing patient samples and isolating *B. pseudomallei* is the gold standard for diagnosis of melioidosis, however, it is not an ideal method (10). It takes 7 to 10 days and has a low sensitivity (true positive rate); only about 60% of melioidosis cases are correctly identified via culture (10). This is partially due to the low numbers of bacteria that accumulate in patient blood (~1 CFU/mL) (11). Other diagnostic methods include the indirect hemagglutination assay (IHA) (12), immunochromogenic cassette test (ICT) (13), direct antigen enzyme-linked immunosorbent assay (ELISA) (14), immunofluoresence microscopy (IFA) (15), and polymerase chain reaction (PCR) (11). Much of the population in endemic regions is seropositive making IHA, ICT, and direct antigen ELISA very inaccurate. IFA and PCR are unreliable, again due to the low levels of bacteria that accumulate in patient blood. Additionally, the heme and human DNA found in blood can inhibit PCR (16). Rapid and accurate diagnosis is critical; delayed treatments allow the bacteria to disseminate to immune privileged sites and are associated with a higher likelihood of patient relapse (7, 17).

B. pseudomallei contains several chromosomally encoded genes that make it inherently resistant to the most commonly prescribed antibiotics, including macrolides, polymyxins, aminoglycosides, cephalosporins, and penicillins (17). Resistance mechanisms include exclusion of antibiotics, efflux of antibiotics, and enzymatic inactivation of the antibiotic (18). *B. pseudomallei* can even delete parts of its genome to develop additional antibiotic resistances during treatment. For example, during the course of ceftazidime treatment, *B.*

pseudomallei can delete a gene encoding the penicillin-binding protein 3, rendering it resistant to ceftazidime (19). The bacterium has multiple antibiotic tolerance mechanisms, including being an intracellular pathogen and possessing the ability to form biofilms (18). Due to the plethora of resistance strategies employed by *B. pseudomallei*, the current treatment regimen is complex, requiring multiple classes of antibiotics. This regimen is extremely difficult to complete, which explains the high lethality and relapse rates in resource-limited environments. The current recommendations for treatment of acute melioidosis require intravenous ceftazidime (or a carbapenem) every 12 hours for at least 2 weeks to treat the initial infection, followed by oral co-trimoxazole and doxycycline, every 12 hours for at least 20 weeks in order to prevent relapse (20).

There are currently no licensed vaccines for *B. pseudomallei* infection. Ongoing approaches in development include subunit vaccines (21), attenuated live microorganisms (22), inactivated whole cells (23), *B. pseudomallei* DNA (24), membrane vesicles (25), and glycoconjugates (26, 27). Many of the vaccines in development show promise and can prolong the mean time-to-death in animal models, however, to date, none of these vaccine formulations have been able to induce sterilizing immunity (as *B. pseudomallei* is still cultured from internal organs).

Virulence factors and host response to *B. pseudomallei*

B. pseudomallei has adapted to survive in a wide variety of environments and hosts. It can grow at a wide pH range or lay dormant in times of nutrient deficiency and reawaken several years later (28, 29). *B. pseudomallei* resists the classical complement pathway and produces many extracellular effector molecules that allow it to thrive as an intracellular pathogen, including proteases, lipases, and phospholiphases (30). It also produces effector molecules that help it avoid host immune responses, including peroxidase and superoxide dismutase, which allow it to resist respiratory burst and reproduce inside macrophages and neutrophils (31). These effector molecules are delivered with bacterial type III and type VI secretion systems (32, 33).

Another very important virulence factor is the *B. pseudomallei* capsule. The bacterium is encapsulated with a high molecular weight capsular polysaccharide (CPS) comprised of an unbranched homopolymer of 1,3-linked 2-O-acetyl-6-deoxy-β-D-*manno*heptopyranose residues (34). CPS is required for virulence (35), it is a protective antigen (36, 37), and it is actively shed into patient samples during infection (38). It aids in cellular adhesion, inhibits complement, and inhibits phagocytosis (39). There are at least 25 genes in the CPS operon that encode for sugar biosynthesis, lipid biosynthesis, sugar transporters, and glycotransferases. Knockout of a subset of CPS biosynthetic genes results in a *B. pseudomallei* mutant that is severely attenuated (40, 41).

<u>Capsules</u>

Capsules are a common virulence factor among many pathogenic bacteria and yeast, including *Neisseria meningitidis* (42), *Klebsiella pneumoniae* (43), *Haemophilus influenzae* (44), and *Cryptococcus neoformans* (45). Most capsules are comprised of polysaccharides. One notable exception is *Bacillus anthracis*, which is encapsulated with a polypeptide (poly-γ-D-glutamic acid) (46). Capsular structures are diverse and vary in sugar composition; however, they are all generally high molecular weight antigens comprised of several repeating epitopes.

The evolution of capsule development was likely the result of environmental selection; encapsulation aids in surviving hostile conditions. Capsular material is generally hydrophilic and prevents desiccation (47), antiphagocytic and prevents uptake by amoeba (47). Capsules are generally large and dense, making them antiviral; bacteriophages cannot easily penetrate capsules to interact with surface receptors (47). Degradation of the capsule in phage-resistant *Streptococcus pneumoniae* renders the bacterium phage-sensitive (48).

These same factors contribute to bacteria survival in patients; capsules are almost always virulence factors. For example, removal of the capsule from *K. pneumoniae* renders the bacterium harmless at otherwise lethal doses in a murine model of *K. pneumoniae* pulmonary infection (43). Capsules are antiphagocytic and prevent uptake by macrophages. They prevent complement

deposition on the bacterial surface and shield pathogen-associated molecular patterns (PAMPs) from the innate immune system (43).

Antibodies that target capsules are opsonic and protective in many cases, including *B. pseudomallei* infection. Antibodies reduce the capsule charge, making it less hydrophilic. This increases complement deposition and phagocyte uptake; phagocytes are assumed to be hydrophobic and antibodies lessen the repulsion between the two (47). However, capsular structures are only weakly immunogenic and do not elicit a robust, persistent humoral immune response. Capsular polysaccharides are T cell-independent type-2 antigens that activate B cells by multivalent cross-linking of antigen receptors (49). Antibodies generated this way are sialylated, causing them to interact with both the bacterium and the immune system in a very weak manner (50).

B. pseudomallei as a potential bioweapon

Due to its high mortality rates and inherent resistance to common antibiotics, the CDC and HHS have classified *B. pseudomallei* as a Tier 1 Select Agent with a high bioterror potential. *B. pseudomallei* has never been weaponized, but the concern is not unfounded. It is believed that many countries have previously had an interest in biological weapons incorporating *B. pseudomallei*, including the former USSR, the USA, and Egypt (1). Additionally, a closely related species, *B. mallei,* has been used as a bioweapon on multiple occasions. During World War I, the Central Powers used *B. mallei* to infect Russian horses with great effect (1). During World War II, the Japanese

intentionally infected human prisoners of war and successfully developed a system to contaminate water supplies with *B. mallei* (1). The bacterium has been used as recently as 1984 in the Russian war in Afghanistan (51).

Antibodies

Antibodies are a structurally diverse group of glycoproteins used by the immune system to identify potential threats. They assist the immune system by binding to an antigen and neutralizing it (52, 53), tagging it for complement (54), or assisting in phagocytosis (55, 56). Also known as an immunoglobulin (Ig), antibodies contain binding regions, called paratopes, which bind to very specific targets called epitopes. An epitope is a structurally unique 3D molecular conformation found on an antigen. Antigens can be almost anything, but they are most commonly foreign microbes or molecules. There are some autoimmune disorders where antibodies target "self" antigens (i.e. rheumatoid arthritis) (57). Paratopes and epitopes are analogous to locks and keys; each paratope can (usually) bind to just one epitope.

Two types of lymphocytes secrete antibodies: B cells and memory cells. B cells are coated with membrane-bound antibodies, called B cell receptors (BCR), which allow them to bind specific antigens and produce antibodies against those antigens. BCR:antigen binding is not enough to stimulate antibody production; the B cell must also receive secondary signals. Secondary signals can come from a T cell (T cell-dependent activation), from the B cell's own toll-like receptors (T cell-independent type-1activation) or from the antigen cross-linking several

BCRs in a multivalent fashion (T cell-independent type-2 activation) (58-60). Secondary signals are a regulatory mechanism that helps prevent B cells from making antibodies to "self" antigens (i.e. autoimmune disorders). Memory cells are a subset of B cells that expand upon reinfection and produce high concentrations of antibody to fight repeating infections.

Antibodies are Y-shaped molecules composed of two light chains and two larger heavy chains (Fig. 1). The tip of each arm is composed of the variable heavy (V_H) and variable light (V_L) chains. Together, these make up the variable region (F_V), which designates the paratope of the antibody. There is incredible paratope diversity with over 10^9 possible combinations available (61). The rest of the antibody is made up of the constant light chain (C_L) and the constant heavy 1, 2, and 3 chains (C_H1, C_H2, C_H3). The constant domain determines the antibody's isotype. There is significantly less diversity in the constant region; in humans there are just five isotypes (IgM, IgD, IgG, IgA, and IgE). Each isotype contributes to immunity in a unique manner. For example, IgA antibodies are usually found in mucosal membranes while IgG antibodies are usually found in serum (62, 63).

Additionally, IgG has four subclasses (IgG_1, IgG_2, IgG_3, IgG_4) and IgA has two subclasses (IgA_1, IgA_2) (64). Antibody subclasses have identical F_V regions, but slightly different heavy chain constant regions (Fig. 2). This means that subclass switch antibodies all have the same paratope, and thus bind to the exact same epitope, but with different binding characteristics and effector functions. For example, human IgG_3 F_C regions interact strongly with complement

and phagocytic monocytes to greatly increase inflammation (65). Conversely, human IgG_4 F_C regions do not bind complement and interact with inhibitory receptors that dampen inflammation (65). Moreover, recent data has shown that human IgG_1 antibodies are the only human subclass that can crosslink F_C regions to increase immune activity (66).

Antibodies can be generated *in vivo* against specific targets by immunizing an animal with an antigen and stimulating that animal's immune system. The animal will make polyclonal antibodies (pAbs) that can be purified from serum. PAbs are isolated as a mixture of antibodies produced from different circulating B cells and therefore can be of varying isotypes and subclasses. PAbs are a combination of several unique antibodies to a single antigen that can bind to multiple epitopes on the antigen. Because pAbs come from multiple B cell clones in vivo, there can be significant batch-to-batch variability, which can make pAbs difficult to characterize; however, this can also be of benefit. For example, pAbs can still bind to antigens that have minor alterations (i.e. glycosylation) because they cover multiple epitopes (67).

Conversely, monoclonal antibodies (mAbs) are produced from a single cell line and bind to just one epitope on the antigen. This makes them highly specific, reduces the chance of cross-reactivity, and makes them simpler to characterize. Additionally, mAbs can be screened based on isotype and affinity, which may be important depending on the downstream applications, such as therapeutics. For example, an IgG antibody is preferable when targeting a blood borne pathogen

because IgG is abundant in serum, while an IgA would be used to target pathogens found in the mucosal membranes. However, this high specificity comes at a cost: mAbs take much longer to generate, require more technical skills to generate, and are much more expensive to produce (67). MAbs are highly desirable for applications when high specificity and reproducibility are important, like pharmaceuticals. There are currently several mAb therapies available, including treatments for rheumatoid arthritis (68), leukemia (69), and human respiratory syncytial virus (RSV) (70).

MAbs can be generated by harvesting the animal's B cells from the spleen. B cells cannot survive for long outside of the spleen and must be immortalized through a fusion with a mouse myeloma (tumor) cell (71). Fused cells of this type are called hybridomas. Hybridomas are isolated at single cell concentrations by limiting dilutions to ensure monoclonality before being grown in bioreactors to mass produce mAbs for purification.

Active and passive immunity

Due to their protective nature, there has been a strong interest in using antibodies to prevent and treat disease. Vaccines are a form of active immunity where the immune system is primed to generate a persistent antibody response against specific pathogens; in the event of infection, the immune system has immunological memory and can rapidly fight the disease. Vaccines can be as simple as introducing heat-killed microorganisms or attenuated live microorganisms, like the polio vaccine (72, 73). However, sometimes it is

undesirable to inoculate a person with whole cell bacteria because of toxins found in the cell membrane (i.e. lipopolysaccharides). In these scenarios, a vaccine may be comprised of just one or two subunits of the pathogen. Toxoids are inactivated toxins and are common subunit vaccines (i.e. tetanus). Capsular polysaccharides (CPS) are also commonly used to generate subunit vaccines. As previously mentioned, capsules by themselves are T cell-independent type 2 antigens, thus weakly immunogenic and unable to elicit a strong humoral immune response. Therefore, a capsule is conjugated to an immunogenic toxoid or protein, transforming it into a T cell-dependent antigen, to elicit a potent and persistent humoral immune response. For example, the *Haemophilus influenzae* type 2 (Hib) vaccine is a conjugate of the capsular polysaccharide of *H. influenzae* to tetanus toxoid (74).

Passive immunization is the transfer of antibodies from one individual to another and can be used to treat disease when there is insufficient time for the infected patient's immune system to develop antibodies on its own. Immunity via passive immunization is temporary; antibodies have a half-life of about 3 weeks and the recipient does not develop immunological memory (75). Passive transfer of antibody occurs naturally between a mother and offspring while the immune system is still developing. Antibodies are transferred across the placenta to protect the unborn fetus; after pregnancy, antibodies are transferred through breast milk. Passive immunity can be artificially induced by transferring antibodies from an immunized donor or animal, in the form of serum or purified

antibody, to a non-immunized patient. For example, sera from patients who survived an Ebola virus infection can be used to treat infected individuals because antiserum potentially contains protective antiviral antibodies (76). Patients receiving antiserum have a risk of developing serum sickness, a potentially life-threatening allergic reaction to other proteins found in serum that is not their own (77). One way to avoid serum sickness is to passively transfer purified monoclonal antibodies.

Lateral Flow Immunoassay

In addition to preventing and treating disease, antibodies can be used to diagnose disease. Due to their highly specific binding capabilities, antibodies can be used to determine exactly what pathogen is infecting a patient in order to provide a specific and targeted treatment. Currently, there are several types of diagnostic tests using antibodies, including enzyme-linked immunosorbent assays (ELISA), immunohistochemistry (IHC), and lateral flow immunoassays (LFI). The present study will focus on the LFI.

LFIs are rapid, single-use, point-of-care (POC) diagnostics. They require minimal amounts of patient sample for testing. LFIs are very user-friendly, requiring minimal equipment and training to operate effectively. They are inexpensive and extremely robust, in that they can be stored in high temperature and humidity settings without loss of potency (78). The most well known LFI is the home pregnancy test (79). LFIs confirm that presence or absence of an analyte (antigen) associated with the condition; in the case of the home

pregnancy test the LFI confirms the presence of human chorionic gonadotropin in the urine of pregnant women.

The LFI quickly moves a liquid sample containing the analyte of interest through 4 zones: i) sample application pad, ii) sample conjugation pad, iii) test & control lines, and iv) absorbent pad (Fig. 3). The sample conjugation pad and test & control lines are characterized by antibodies that interact with the analyte of interest in a specific manner to ultimately create a sandwich assay; zones are sequentially connected with a porous membrane that facilitates liquid flow. Membranes come in various pore sizes and materials, including nitrocellulose (79), nylon (80), or polyethylene (81); membranes are chosen based on the size and characteristics of the analyte being tested. A brief overview of the zones will follow.

The patient sample is first applied to the sample application pad. Capillary action draws the analyte to the sample conjugate pad where it can interact with labeled antibodies. Labels must be small so they do not obstruct flow through the membrane and must be detectable. Common labels include colloidal gold (79), carbon black (82), and europium (83). Colloidal gold and carbon black have the advantage of being visually detectable with the naked eye. Europium is fluorescent and requires a fluorometer, however, it is generally more sensitive (83).

Capillary action continues and the analyte:labeled antibody complex is drawn to an immobilized antibody at the test & control lines. This creates an

antibody:analyte:labeled-antibody sandwich that can detected. The intensity of the response is directly proportional to the amount of analyte in the sample. If there is no analyte in the sample, the labeled-antibody will pass right over the immobilized antibody and no visual sandwich will be made. A mAb that binds to other mAbs is immobilized at the control to confirm the liquid has flowed all the way through the strip. The total test time is about 10 minutes (83).

<u>**Summary**</u>

B. pseudomallei is an opportunistic pathogen and the causative agent of melioidosis, a disease that causes significant morbidity and mortality in endemic regions. The bacterium is considered to have high bioterror potential due to its ease of culture from the soil, the relatively small numbers of bacteria needed for infection, and its resistance to commonly prescribed antibiotics. There are currently no vaccines available to prevent *B. pseudomallei* infection and current diagnostic methods are cumbersome and inaccurate. Like many other pathogenic microorganisms, *B. pseudomallei* surrounds itself with a high molecular weight capsular polysaccharide (CPS) that contributes greatly to bacterial virulence and pathogenicity. The CPS is shed into infected patient serum and urine.

Antibodies are highly specific immune molecules that are generated in response to pathogen infection in order to neutralize and clear threats. Due to their highly specific and protective nature, we can use antibodies to both diagnose and treat disease. The present work describes the generation of a

library of mAbs, including 2 full subclass-switch IgG families, targeting the CPS of *B. pseudomallei* for the diagnosis and treatment of melioidosis. Each mAb has been thoroughly characterized to facilitate the selection of mAbs that may provide protection against *B. pseudomallei in vivo*. In addition, our work has lead to the development of the Active Melioidosis Detect™ Lateral Flow Immunoassay for the rapid diagnosis of melioidosis (AMD LFI). The AMD LFI is currently undergoing validation at a variety of locales across the globe in both clinical and environmental settings where it is being tested for sensitivity and stability.

Figure 1. Antibodies are comprised of two heavy chains and two light chains. The heavy chain consists of 3 constant domains and 1 variable domain; the light chain consists of 1 constant domain and 1 variable domain. Together, the variable heavy chain and the variable light chain make up the variable region (F_V). The F_V region determines which antigens the antibody can bind to.

Figure 2. Antibody subclasses have identical variable regions and all bind to the same epitope, but have different heavy chain constant regions, and thus different effector functions.

Figure 3. Schematic of a lateral flow immunoassay (LFI). A liquid sample containing the analyte of interest is applied to sample pad and capillary action pulls the sample through to the conjugate pad. Here, gold-labeled antibodies bind with the analyte. Next, the analyte:labeled antibody complex flows to the test line where immobilized antibodies will interact with the analyte to create a sandwich assay, which creates a red line for a positive result.

Chapter 1

Immunoglobulin G F$_C$ region affects the binding of monoclonal antibodies to the capsular polysaccharide of *Burkholderia pseudomallei*

Michael J. Dillon, Rachael A. Loban, Dana E. Reed, Peter Thorkildson, Paul J. Brett, Mary N. Burtnick, Richard A. Bowen, and David P. AuCoin*

Department of Microbiology and Immunology, University of Nevada School of Medicine, Reno, Nevada, 89557

Department of Cellular and Molecular Biology, University of Nevada School of Medicine, Reno, Nevada, 89557

*Corresponding author. Mailing address: Department of Microbiology and Immunology/320, University of Nevada School of Medicine, 1667 North Virginia Street, Reno, NV 89557.
Phone: (775) 784-4128. Fax: (775) 327-2332. E-mail: daucoin@medicine.nevada.edu

Abstract

Immunoglobulin G3 (IgG_3) is the predominant antibody isotype and subclass in response to polysaccharide antigens in mice. This specific subclass seems better suited than other subclasses to bind to polysaccharide antigens commonly displayed on bacteria and yeast. The improved binding appears to be due to the fact that murine IgG_3 antibodies have increased avidity through fragment crystallizable (F_C) region cross-linking that is not seen in other IgG antibody subclasses. In order to further investigate this phenomenon, we have analyzed the binding characteristics of two IgG monoclonal antibody (mAb) subclass families that bind to the capsular polysaccharide (CPS) of *Burkholderia pseudomallei*. The first subclass family originated from an IgG_3 hybridoma cell line (3C5); the second family was generated from an IgG_1 cell line (2A5). When the F_C region of the 3C5 IgG_3 is removed by proteolytic cleavage, the resulting $F(ab')_2$ fragments exhibit significantly decreased affinity compared to the full-length mAb. Similarly, when the F_C region is subclass-switched, the resulting IgG_1, IgG_{2b}, and IgG_{2a} antibodies all exhibit significantly decreased affinity and protection in a murine model of pulmonary melioidosis. This dramatic decrease in affinity and protection is not seen when the parent 2A5 IgG_1 is switched to an IgG_{2b} or IgG_{2a}, strongly suggesting the change in affinity is related to the IgG_3 F_C region.

Introduction

Polysaccharide capsules are known to contribute to bacterial virulence by inhibiting complement activation and preventing phagocytosis (1-5). They are high molecular weight antigens with repeating epitopes that are displayed on the bacterial and fungal cell surface (6-9). Anti-capsular antibodies are an important mechanism for host defense, thus capsules are appealing vaccine candidates; however, polysaccharide antigens do not illicit a robust humoral immune response by themselves. Robust humoral immunity is induced in a T-cell dependent (TD) manner (10), however, polysaccharides can bypass this mechanism and stimulate B-cells by cross-linking multiple cell surface antigen receptors. T-cell independent (TI) responses produce a much weaker humoral immune response (11). One way to generate lasting humoral immunity to a polysaccharide is to conjugate it to a highly immunogenic protein or toxoid (12-14). For example, the Haemophilus influenzae capsule elicits a much stronger immune response when it is conjugated to tetanus toxoid (12).

IgG subclass in response to polysaccharide antigens is restricted. In humans, IgG_2 is the predominant antibody response to polysaccharide antigens (15); in rats, IgG_{2c} is the predominant response (16). In mice, IgG_3 is produced almost exclusively to polysaccharide antigens, while the other subclasses are generated in response to other antigens (17-19). For example, murine IgG_1 is restricted to protein antigens (18). Subclass

families are comprised of antibodies that have identical variable regions (F_V) but different heavy chain constant regions; at a very low frequency, antibodies spontaneously convert into different downstream subclasses through constant heavy chain gene recombination in vivo. We have adapted a technique to isolate subclass-switch hybridoma clones in vitro, which is based on sequential sib selection (20, 21). This allows for efficient study of subclass-switch mAb families.

Seminal research by Greenspan and colleagues established the enhanced binding of murine IgG_3 to polysaccharides over that of non-IgG_3 subclass-switch mAbs containing identical variable regions (22-24). Specifically, it was shown that the antibodies in a murine IgG subclass family ($IgG_3 \rightarrow IgG_1 \rightarrow IgG_{2b}$), which did not include an IgG_{2a}, interact with the same Group A streptococcal antigen in very different ways. Murine IgG_3 bound cooperatively and thus possessed a higher affinity than IgG_1 or IgG_{2b}. Similarly, IgG_3-derived $F(ab')_2$ fragments did not show cooperative binding and bound with a much lower affinity, similar to that of the IgG_1 and IgG_{2b} (22). In an additional study, Cooper et al. generated a partial subclass family ($IgG_3 \rightarrow IgG_1$) to the lipopolysaccharide (LPS) of *Pseudomonas aeruginosa*. IgG_3 showed superior binding to both purified LPS and whole bacteria (24). Similarly, the IgG_3 variant of a complete subclass family exhibits greater binding affinity to the capsular polypeptide of *Bacillus anthracis* (21) compared to all three other subclasses. Reduced

binding affinity was a result of alterations in the C_H2 and C_H3 domains, which comprise the F_C region in IgG molecules. When altering this same murine IgG_3 F_C region by engineering human chimeric antibodies (chAbs), the resulting chAbs have significantly reduced binding affinities for the capsular polypeptide (25). Taken together, this data suggests that changes in the F_C region can alter antibody-antigen interactions.

The goal of this study was to determine if the murine IgG_3 F_C region contributes to the affinity of antibodies binding to the capsular polysaccharide (CPS) of *Burkholderia pseudomallei.* Subclass-switch families of mAb 3C5 (IgG_3➔IgG_1➔IgG_{2b}➔IgG_{2a}) and mAb 2A5 (IgG_1➔IgG_{2b}➔IgG_{2a}) were generated. Both mAb families bind CPS; mAb 3C5 was isolated from a mouse immunized with heat-killed whole *B. pseudomallei* cells (26). MAb 2A5 was generated from a mouse immunized with CPS covalently linked to bovine serum albumin (BSA); this glycoconjugate was previously shown to induce high titers of CPS-specific IgG antibodies in mice (14). MAb 3C5 is a relatively high affinity murine IgG_3 that has been shown to provide passive protection in a murine model of pulmonary melioidosis (27). MAb 2A5 is a murine IgG_1 with a similar affinity to mAb 3C5 IgG_3.

The results of this study suggest that antibody affinity is an important factor in protection, and that the IgG_3 F_C region significantly contributes to affinity through avidity when binding to antigens that contain

repeating epitopes (such as polysaccharides). Removal of the F_C region from IgG_3 mAb 3C5 by proteolytic cleavage substantially decreases the affinity of the resulting $F(ab')_2$ fragment. Similarly, switching the F_C region from an IgG_3 to an IgG_1, IgG_{2b}, or IgG_{2a} results in a substantial decrease in affinity. These results were determined via surface plasmon resonance (SPR), and also confirmed with a direct antigen binding ELISA. Furthermore, IgG_3 mAb 3C5 provides superior protection over the subclass-switch variants in a murine model of pulmonary melioidosis. This change in affinity and drop in protection is not seen when IgG_1 mAb 2A5 switches to an IgG_{2b} or IgG_{2a}. Taken together, the IgG_3 F_C region contributes to antibody binding to *B. pseudomallei* CPS resulting in increased affinity and superior protection in a murine model of pulmonary melioidosis.

Materials and Methods

Immunization of mice and production of mAbs. Generation of mAb 3C5 IgG_3 has been described (27). Briefly, *B. pseudomallei* strain 1026b was grown overnight at 37 $^{\circ}$C in brain heart infusion broth. Bacteria were heat inactivated at 80 $^{\circ}$C for 2.5 hours. BALB/c mice were immunized via intraperitoneal (i.p.) injections with 2 x 10^8 heat-inactivated bacteria every two weeks for eight weeks total. An ELISA was used to assess antibody titers to *B. pseudomallei*. A final boost was administered three days prior to splenectomy. Hybridoma cells were produced as previously described (28). Western blot analysis was performed to identify hybridoma cell lines that were producing mAbs reactive with purified CPS.

MAb 2A5 IgG_1 was produced using CPS conjugated to bovine serum albumin (BSA) (14). BALB/c mice were immunized via i.p. injections with 5 μg of CPS-BSA every two weeks, for six weeks total. Antibody titers were measured via ELISA (see below) and hybridoma cell lines were generated as above.

A modified protocol based on the method of Spira et al. (20) was used to isolate subclass-switch families as previously described (20, 21). Briefly, subclass-switch hybridomas were identified via ELISA and plated at limiting dilution until the cell line was completely sublined (20). Cell lines were grown in Integra CL 1000 culture flasks (Integra Biosciences) with RPMI media containing 4.5 g glucose, 4 mM L-glutamine, 50 μM 2-

mercaptoethanol, 20 mM HEPES, 1 mM sodium pyruvate, and 15% fetal bovine serum (FBS) (low IgG). Antibodies were purified by affinity chromatography over a protein-A column.

F(ab')$_2$ fragments. F(ab')$_2$ fragments were generated from digestion of full-length mAbs with pepsin from porcine gastric mucosa (Sigma). Summarily, mAbs (5 mg/mL) were incubated with shaking at 37 °C for 30 min with pepsin at a final concentration of 0.2 μg/mL in 20 mM NaOAc, pH 4.4. Next, 10% (v/v) of Tris (2M) was used to stop the reaction. F(ab')$_2$ fragments were purified over a Superose 12 (GE Healthcare) molecular sieve column.

MAb variable region sequencing. MAb heavy and light chain variable regions were sequenced as previously described (21). Briefly, total mRNA was isolated from each hybridoma cell line with a RNeasy Mini Kit (QIAGEN). cDNA was synthesized using a First Strand cDNA Synthesis Kit (Thermo Scientific) and amplified with a Mouse Ig-Primer Set (Novagen). PCR products were TA cloned into the pGem-T vector (Promega), and sequenced at the Nevada Genomics Center. Two independent clones were sequenced for each experiment.

Western blot. One μL of a 10x concentrated *B. pseudomallei* 1026b lysate, 1.1 x 10^5 cfu of *B. mallei* China 7 (BEI), 8 x 10^6 cfu of *B. thailandensis* E264 (BEI), or 0.5 μg purified CPS were incubated with 1 volume of proteinase K at 3.3 mg/mL for 1 hr at 60 °C. Next, samples were

separated by sodium dodecyl sulfate-12% polyacrylamide gel electrophoresis (SDS PAGE) (BioRad) at 160 V for 1 hr, followed by transfer to a nitrocellulose membrane (BioRad) via a TransBlot Turbo (BioRad). Membranes were blocked in TBS+0.1% Tween 20, 5% milk overnight at 4 °C (blocking solution). Membranes were then probed with mAbs at 0.1 μg/mL diluted in blocking solution for 1 hr while rocking at room temperature. Membranes were washed 3 times for 15 min with TBS+0.1% Tween 20 and mAb binding was detected with peroxidase-conjugated goat anti-mouse kappa chain antibody (Southern Biotech) diluted 1:10,000 in blocking solution and incubated for 30 min at room temperature. Membranes were washed 3 additional times and binding was detected with SuperSignal West Femto Chemiluminescent Substrate (Pierce). Binding was visualized with a Chemidoc imaging system (BioRad).

Surface plasmon resonance. Binding affinity was determined by surface plasmon resonance (SPR) with a BIAcore X100 (GE Healthcare). Purified CPS was benzoquinone-activated and conjugated to biotin as previously described (29), and immobilized onto a streptavidin (SA) sensor chip at 30 response units (RU). A second flow cell was unmodified and used for reference subtractions. Affinity was evaluated with mAbs diluted in HBS-EP+ running buffer (10 mM HEPES, 150 mM NaCl, 3 mM EDTA, and 0.05% surfactant P20) at a range of 0-333 nM or 0-3300 nM. Two-fold

serial dilutions of mAb were injected over the immobilized CPS at 30 μL/min for 60 s, followed by 120 s of passive dissociation. The sensor chip surface was regenerated between each concentration with 10 mM HCl, pH 1.5. Dissociation constants (K_D) were calculated using BIAevaluation software (GE Healthcare).

ELISA. Polystyrene plates (Thermo Scientific) were coated for 90 min at 37°C with 0.005% (w/v) Poly-L-Lysine (Sigma) diluted in PBS. Plates were washed with PBS and incubated overnight with 4 μg/mL of purified CPS (14). Next, plates were washed with PBS+0.05% Tween 20 and blocked with PBS+0.05% Tween 20, 5% milk (blocking solution) at 37 °C for 90 min. MAbs (or mouse sera) were two-fold serially diluted across the wells in blocking solution (from 2000 μg/mL) and the plates were incubated at 37 °C for 90 min. MAb binding was detected with peroxidase-conjugated goat anti-mouse kappa chain antibody (or peroxidase-conjugated goat anti-mouse IgG antibody) (Southern Biotech) diluted in blocking solution at 1:10,000 and incubated for 90 min, followed by TMB peroxidase substrate (KPL) for 30 min. The enzymatic reaction was stopped by adding 100 μL of 5% o-phosphoric acid to each well and the optical density was determined by measuring absorbance at 450 nm. Each experiment was completed in duplicate. To calculate the antibody concentration that induces a response halfway between baseline and maximum (EC_{50} value),

a four-parameter logistics curve fit was applied using Sigma Plot 11.0 (Systat Software Inc.).

Animal protection studies. Intranasal challenge experiments were performed as previously described under ABSL-3 conditions (27). Briefly, six week old female BALB/c mice were injected with 1 mg of mAb by the i.p. route 18 h prior to challenge. *B. pseudomallei* 1026b at 7100 cfu/0.1 mL (21 LD_{50}) was introduced to each mouse by the intranasal (i.n.) route. Mice were monitored 42 days post-infection for weight loss, lack of activity, matted fur, and other clinical symptoms. Statistics were performed using a log-rank (Mantel-Cox) test with an adjusted Bernferroni-corrected threshold using GraphPad Prism 6.0. Infected control mice were administered PBS instead of mAb. Survivors were necropsied and internal organs were examined for abscess growth. Spleens were homogenized in 1 mL of brain-heart infusion (BHI)/10% glycerol and 0.1 mL of the homogenate was plated on a BHI-gentamicin plate.

Ethics statement. All studies were carried out in accordance with the recommendations in the Guide for the Care and Use of Laboratory Animals of the National Institutes of Health. The Animal Care and Use Committees at the University of Nevada, Reno (Protocol A07/08-16) and at Colorado State University (Protocol #09-001A) approved all protocols.

Results

We previously generated the IgG_3 mAb, 3C5, from BALB/c mice immunized with heat-inactivated whole *B. pseudomallei* (26); notably, we generated the IgG_1 mAb, 2A5, in a different manner, from BALB/c mice immunized with purified CPS conjugated to BSA (9). Subclass-switch families of both mAbs were generated with a modified sequential sib selection protocol (20). In order to verify that the heavy and light chain variable regions were identical for all subclasses, total mRNA was isolated from each hybridoma cell line and used for cDNA synthesis and PCR amplification. PCR products were ligated into pGEM-T and sequenced (data not shown).

Western blot analysis was used to verify that all of the generated mAbs bind to CPS. CPS is a high molecular weight antigen comprised of an unbranched polymer of -3)-2-O-acetyl-6-deoxy-β-d-*manno*-heptopyranose-(1- residues that produce a characteristic smear via Western Blot (9). The IgG_3 variant of mAb 3C5 and the IgG_1 variant of mAb 2A5 both bind to the same proteinase K-resistant high molecular weight antigen found in *B. pseudomallei*, *B. mallei* and purified CPS preparations. Additionally, neither mAb binds to *B. thailandensis*, which lacks CPS (30) (Fig. 1). Subclass-switching mAb 3C5 yielded mAbs that bind to CPS via Western blot, but require much higher concentrations to produce similar signal levels (data not shown). Subclass-switching mAb

2A5 generated mAbs that bound to CPS at similar signal levels as the parent IgG_1 (data not shown).

In order to elucidate the relationship between subclass F_C region and mAb binding, the binding kinetics of each mAb were determined by SPR with a BIAcore X100. Purified CPS was conjugated to biotin (29) and immobilized on a streptavidin-coated sensor chip. Total immobilization of CPS was 30 RU. MAbs were injected over a 60 second pulse and a titratable increase in RU was observed (Fig. 2). The steady state model from BIAevaluation software was applied to each graph to determine the dissociation constant for each mAb (Fig. 3). The calculated binding affinity of each mAb is in Table 1. Notably, the subclass-switch variants of mAb 3C5 have much lower affinity for CPS than the parent IgG_3. In order to determine if this was due to the change in F_C region, $F(ab')_2$ fragments were produced from the 3C5 IgG_3; the $F(ab')_2$ fragments had even lower affinity compared to the subclass-switches. Importantly, the calculated binding affinity of the subclass-switch variants of mAb 2A5 remained constant, which led us to believe that, while changes in the IgG_3 F_C region appear to affect affinity, changes in the IgG_1 F_C region do not.

An ELISA was performed to compare the relative antigen binding characteristics of the 3C5 and 2A5 subclass families (Fig. 4). Purified CPS was plated in the solid phase at 4 μg/mL and 2-fold serial dilutions of mAbs were added in the fluid phase starting at 2,000 μg/mL. Each line on

the plot represents a different mAb subclass. The 3C5 subclass-switch mAbs require much higher concentrations to generate the same response as the IgG_3, whereas the 2A5 subclass-switch mAbs all perform similarly to each other. These plots were used to calculate the half-maximal effective concentration value (EC_{50}), which is the antibody concentration that generates a response halfway between the baseline and maximum; smaller values correlate with a higher efficacy (Table 1). The calculated EC_{50} value for the IgG_3 variant of mAb 3C5 was 0.9 μg/mL, whereas the calculated EC_{50} values for the subclass-switch mAbs were well over 10-fold higher. The calculated EC_{50} value of the IgG_1 variant of mAb 2A5 was about 2-fold lower than mAb 3C5, indicating that it has a higher efficacy. Similar to the affinity analysis, the calculated EC_{50} values of the 2A5 subclass variants remained comparable to the parent IgG1.

We previously determined that the IgG_3 variant of mAb 3C5 was protective in a murine model of pulmonary melioidosis, where 75% (6/8) of immunized mice survived inoculation with 15 LD_{50} of *B. pseudomallei* 1026b (27). We wanted to investigate whether a change in F_C region would affect the ability of CPS mAbs to afford protection in vivo, so each mAb was assessed as previously described (Fig. 5) (27). Mice were passively immunized with 1 mg of mAb and subsequently challenged with 21 LD_{50} of *B. pseudomallei* 1026b by the intranasal route. All infected mice showed reduced activity, a decrease in weight, and severe illness (Fig. 6).

The IgG$_3$ variant of mAb 3C5 protected 25% (2/8) of the infected mice with a mean time to death (MTD) of 31 days (Table 2). This appears to contradict our previous study, where mAb 3C5 protected 75% of infected mice; however, it is important to note that the mice in this challenge received a much higher dose of bacteria than in our original study. The increased bacterial load dramatically accelerated how quickly the control mice got sick; in our first study, control mice survived until day four, whereas in the current study control mice survived only to day 2.

The IgG$_1$ and IgG$_{2a}$ variants of mAb 3C5 provided similar levels of protection to the IgG$_3$ but with much shorter MTDs of 4 and 4.5 days respectively; the IgG$_{2b}$ variant offered slightly higher protection than the IgG$_1$ and IgG$_{2a}$ at 37.5% (3/8) and a MTD of 16 days. Similar to the trends seen in the SPR/affinity and ELISA experiments, all of the 2A5 subclass-switch mAbs provided similar levels of protection; in fact, the 2A5 mAbs all offered increased levels of protection compared to the 3C5 family, even the IgG$_3$ variant (Table 2).

In addition to survival, each mAb's effect on spleen cfu and abscess formation was determined. Spleen cfu were recorded and splenic abscesses were counted in surviving mice only. Both were assumed to occur in mice that died before day 42 in order to allow for statistical analysis (Table 2). 87.5% (7/8) of the mice immunized with the IgG$_3$, IgG$_1$, and IgG$_{2a}$ variants of mAb 3C5 had detectable spleen cfu; only 62.5%

(5/8) of the mice immunized with the IgG_{2b} variant showed spleen cfu. None of the survivors developed splenic abscesses as determined by gross examination. Of the mice immunized with the 2A5 subclass antibodies, 50% (4/8) of the mice immunized with the IgG_1 variant had spleen cfu, while 71.4% (5/7) and 62.5% (5/8) of the mice immunized with the IgG_{2b} and IgG_{2a} variants showed spleen cfu, respectively. Only 2 of the surviving mice immunized with the IgG_1 variant developed apparent splenic abscesses.

Discussion

Many pathogenic microorganisms produce capsular structures, including *Haemophilus influenzae* (31), *Neisseria meningitidis* (32), *Bacillus anthracis*, and *Cryptococcus neoformans* (33). These capsules are comprised of polysaccharides or, in the case of *Bacillus anthracis*, a polypeptide (34). Capsules are antiphagocytic and are generally required for virulence (35). Antibodies that target capsules are opsonic and protective in many cases (35). As such, capsules are ideal vaccine targets, however, most capsular polysaccharides do not elicit a strong immune response, especially in infants and young children (36). Capsular polysaccharides are high molecular weight antigens comprised of several identical repeating units, making them T-cell independent type 2 antigens (TI-2) (37). They can activate B-cells by multivalent cross-linking of B-cell antigen receptors, which produces a very specific antibody response (11). Mice generally produce IgG_3 in response to capsular polysaccharides (17-19); humans generally produce IgG_2 (15). As such, it is important to elucidate the immunochemistry between antibodies and microbial capsules so that we may develop effective vaccines and immunotherapeutics that elicit the appropriate humoral response against encapsulated pathogenic microbes.

There have been multiple studies showing mAbs can provide passive protection in a murine model of melioidosis, however, there have

been no studies to date comparing different antibody subclasses (38-43). Subclass-switch families are antibodies with identical F_V regions but different heavy chain constant regions, thereby making them invaluable for determining how the F_C region contributes to binding. This study builds on previous work showing that antibodies subclass-switch antibodies bind to their target with a different specificity and affinity, despite having identical F_V regions (23, 44). In one study, altering the C_H1 domain of antibodies targeting HIV-1 gp41 resulted in variable-region identical mAbs that bound to completely different epitopes (44). In a separate study, IgG_{2a} derived $F(ab')_2$ fragments bound stronger to *C. neoformans* GXM than the intact IgG_{2a} or even the IgG_3 variant, indicating that structural changes to the C_H1 domain contribute to antibody affinity (45). Additionally, our group has shown that changes in the C_H2 and C_H3 domains can also affect antibody binding affinity. Replacing any of the IgG_3 C_H domains with IgG_{2b} C_H domains greatly reduced the antibody's ability to bind to γDPGA (21).

In the current study, we generated two different subclass-switch families: one that originated from a high affinity IgG_3 mAb (3C5) and one that originated from a high affinity IgG_1 mAb (2A5). Removal of the F_C region of mAb 3C5 by proteolytic cleavage generates IgG_3 $F(ab')_2$ fragments with reduced affinity by SPR and a 300-fold increase in EC_{50} by ELISA. Similarly, subclass-switching mAb 3C5 from an IgG_3 to an IgG_1 results in a 20-fold loss in affinity and twofold increase in EC_{50} values.

Subclass-switching the IgG_1 variant to IgG_{2b} or IgG_{2a} results in antibodies with a similar affinity and binding capacity to the IgG_1. Subclass-switching mAb 2A5 from an IgG_1 variant into an IgG_{2b} or IgG_{2a} variant yields mAbs with similar affinities and EC_{50} values to the IgG_1. Taken together, this strongly suggests that the drop in affinity and binding capacity is related to the IgG_3 F_C region. Altering the F_C region of an IgG_1 mAb does not seem to impact antibody binding.

Previous studies have shown that the IgG_3 variant of mAb 3C5 is protective in an animal model of pulmonary melioidosis (27). To assess if reduced affinity and binding capacity would impact animal protection, we administered groups of mice with mAbs of different subclasses from the same family. As in our previous study, passive immunization with the IgG_3 variant increased survival rates. In the previous study, the IgG_3 variant of mAb 3C5 protected 75% (6/8) of infected mice, while in this study, only 25% (2/8) of infected mice were protected (27). However, it is important to note that the mice in the current study where challenged with more bacteria: 21 LD_{50} (resulting in 7100 cfu/mouse) as compared to 15 LD_{50} (5000 cfu/mouse) in the first study. This increased bacterial load caused control mice to become moribund by day 2; in the first study, control mice survived until day 4.

Passive immunization with the IgG_1 and IgG_{2a} subclass-switch variants provided similar survival rates of 25% (2/8), however, the mice in

these groups had significantly shorter MTD (4 and 4.5 days, respectively) indicating that they were not nearly as effective. These findings are supported by recent results published by our group (21). In this study, mice were immunized with a subclass-switch family of mAbs targeting the capsule of *B. anthracis*. *B. anthracis* has a polypeptide capsule comprised of poly-gamma-D-glutamic acid (γDPGA) that shares many characteristics with polysaccharide capsules, such as being a TI-2 antigen (46). In these studies, only the IgG_3 variant was protective in a murine model of pulmonary anthrax (21).

Next, we wanted to determine if the decreased protection afforded by the different subclasses was due to their reduced affinity or inherently related to mAb subclass. Murine IgG_3 antibodies have the unique ability to cross-link their F_C domains and bind cooperatively; this can even occur between two different IgG_3 mAbs that bind to two independent polysaccharide antigens (47). Cooperative binding does not occur if the F_C region is removed or switched to another subclass (23), and we wondered if cooperative binding was necessary for protection. Mice were passively immunized with the high affinity 2A5 subclass-switch family of mAbs. The IgG_1, IgG_{2b}, and IgG_{2a} variants of mAb 2A5 provided 87.5% (7/8), 71.4% (5/7), and 75% (6/8) protection of infected mice, respectively, indicating that protection is not dependent on IgG_3 F_C-F_C interactions. There were not enough deaths to determine a MTD. Similarly, studies with both *B.*

anthracis and *Cryptococcus neoformans* suggest that non-IgG$_3$ capsule-specific mAbs may be protective (48-51). In a murine model of pulmonary anthrax, both IgG$_3$ and non-IgG$_3$ mAbs significantly increase mouse survival rates (48, 49). Similarly, the higher affinity mAbs afforded more protection than the lower affinity mAb (48). Additionally, in a murine model of cryptococcal meningitis, IgG$_1$ mAbs provide the highest rates of protection, even when the IgG$_3$ variant has a higher affinity (50, 51). In fact, the IgG$_3$ variant can even enhance virulence in some cases (52).

The results of this study show that mAbs targeting the CPS of *B. pseudomallei* are protective in a murine model of pulmonary melioidosis. At this dose (1 mg per mouse), protection is independent of IgG subclass; the high affinity 2A5 subclass mAbs all provided significant levels of protection. One hypothesis for the decreased protective efficacy of the 3C5 subclass-switch mAbs is a decrease in affinity. Subclass-switching of mAb 3C5 from an IgG$_3$ to any other subclass generates an antibody with significantly reduced binding capacity. MAb 3C5 has high affinity as an IgG$_3$ variant; however, this could reflect avidity effects due to F$_C$-F$_C$ crosslinking. Removing the IgG$_3$ F$_C$ via proteolytic cleavage or altering the F$_C$ region via subclass-switching prevents F$_C$-F$_C$ interactions, which reduces the apparent affinity. Meanwhile, mAb 2A5 originates with a high affinity as an IgG$_1$, *without* F$_C$-F$_C$ crosslinking, and thus, did not lose affinity with subclass-switching. This may explain why all of the 2A5

subclass variants were equally protective and the 3C5 variants were less protective and had a much shorter MTD when compared to the IgG_3. IgG_3 is the primary IgG response to polysaccharides in mice (17-19); F_C-F_C interactions may help the antibodies bind more strongly until affinity-matured antibodies of other subclasses can be generated.

In summary, this study suggests that IgG_3 F_C regions play an important role in antibody binding by increasing affinity and avidity. Altering or removing the F_C region reduces antibody-binding capacity and diminishes protection. However, protection is not solely dependent on the IgG_3 F_C region; a murine model of melioidosis indicates that high affinity mAbs of any subclass may be a viable therapeutic for *B. pseudomallei* infection. The mAbs in this study were not able to provide sterilizing immunity, however, they did extend MTD in mice inoculated with a very high dose of *B. pseudomallei*, and therefore, could potentially be used as an adjunct therapy to antibiotics for melioidosis. There have been several melioidosis vaccine studies in animals (53), none of which have resulted in sterile immunity. CPS is a potential vaccine candidate (27, 54), therefore, anti-CPS immunization strategies should prioritize eliciting robust, high affinity antibody titers. Future studies include testing the mAbs in a dose-dependent manner in order to elucidate potential differences between subclasses, and in post-exposure scenarios for the development of a melioidosis immunotherapeutic.

Acknowledgements

Table 1. Summary of antibodies generated for this study.

mAb	IgG Subclass	VH Family	VL Family	K_a ($[\mu M\text{-}s]^{-1}$)[a]	K_d (s^{-1})[b]	K_D (nM)[c]	EC_{50} ($\mu g/mL$)
3C5	IgG$_3$	Vh6	IgK V19/28	0.28	0.0011	73	0.9±0.03
	IgG$_1$	Vh6	IgK V19/28	0.016	0.0024	1,460	18±1.7
	IgG$_{2b}$	Vh6	IgK V19/28	0.027	0.0024	790	12±0.8
	IgG$_{2a}$	Vh6	IgK V19/28	0.043	0.0041	550	12±1.0
	F(ab')$_2$[d]	-	-	0.038	0.0059	2,100	383±130
2A5	IgG$_1$	Vh6	IgK V21	1.8	0.024	43	0.37±0.02
	IgG$_{2b}$	Vh6	IgK V21	1.1	0.012	36	0.36±0.03
	IgG$_{2a}$	Vh6	IgK V21	0.72	0.0093	58	0.76±0.08

[a]Association rate constant   [b]Dissociation rate constant   [c]Disocciation constant   [d]IgG$_3$ F(ab')$_2$
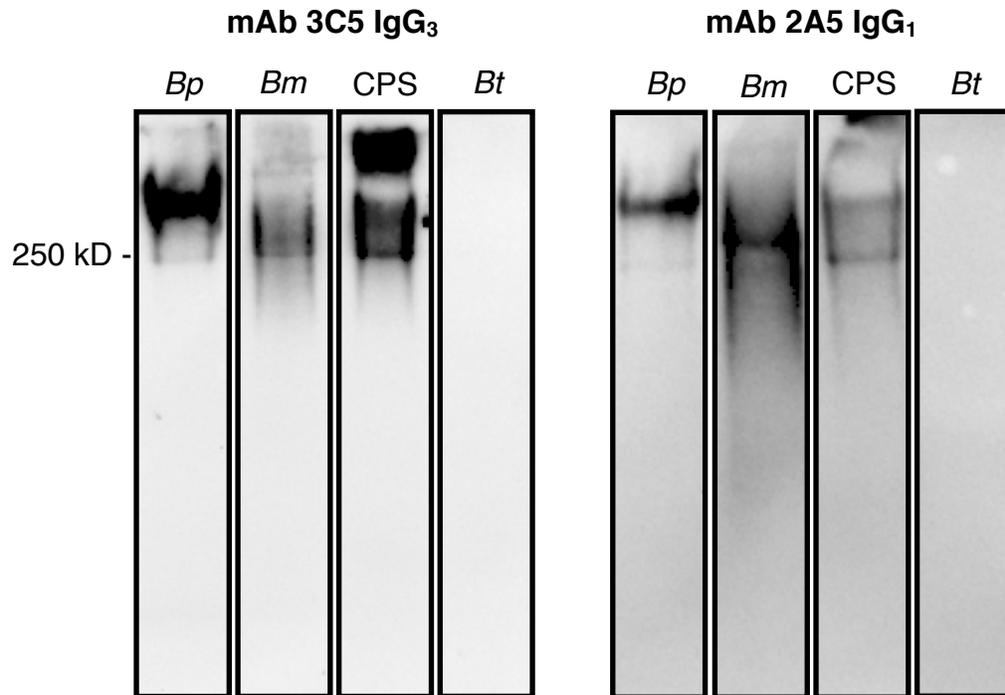
Figure 1. *B. pseudomallei* (*Bp*) 1026b, *B. mallei* (*Bm*) China 7, purified CPS, or *B. thailandensis* (*Bt*) E264 were incubated with proteinase-K, separated by SDS PAGE, and subsequently transferred to a nitrocellulose membrane. Membranes were probed with 0.5 *µ*g mAb and binding was detected with an HRP-conjugated goat anti-mouse kappa chain antibody. MAbs 3C5 (IgG$_3$) and 2A5 (IgG$_1$) bind to a high molecular weight, proteinase-K resistant antigen found in *B. pseudomallei*, *B. mallei*, and purified CPS. MAbs do not interact with *B. thailandensis*, which lacks CPS. The subclass-switch families bind with similar results (data not shown).
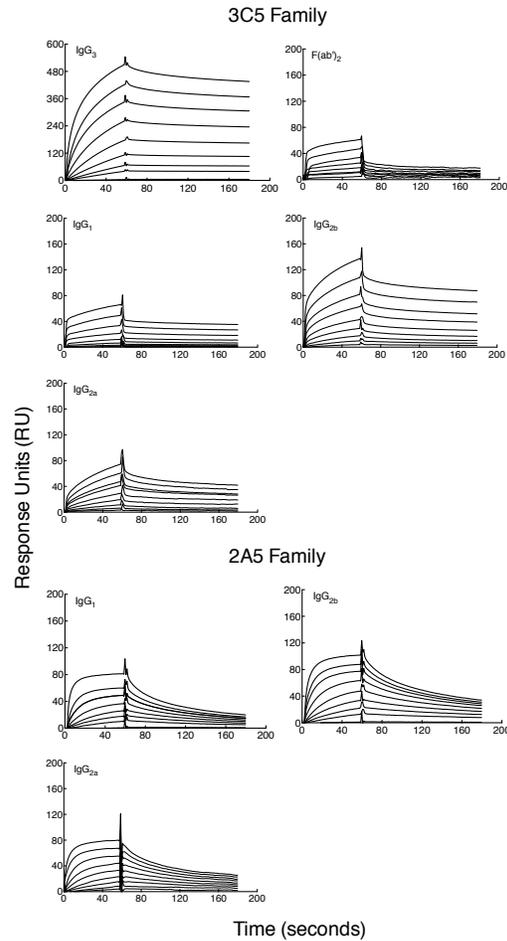
Figure 2. Binding specificity of subclass-switch family mAbs and 3C5 IgG$_3$ F(ab')$_2$ fragments given as a function of response generated over time. A BIAcore X100 instrument was used to determine the affinity of each mAb for CPS. Purified CPS was conjugated to biotin and immobilized on a SA sensor chip. MAb binding was analyzed by injecting eight samples (2-fold serial dilutions (0.33-333 or 12-3,333 nM) for 60 s, followed by 120 s of passive dissociation. Note the magnitude of the response for 3C5 IgG$_3$ compared to all other mAbs.
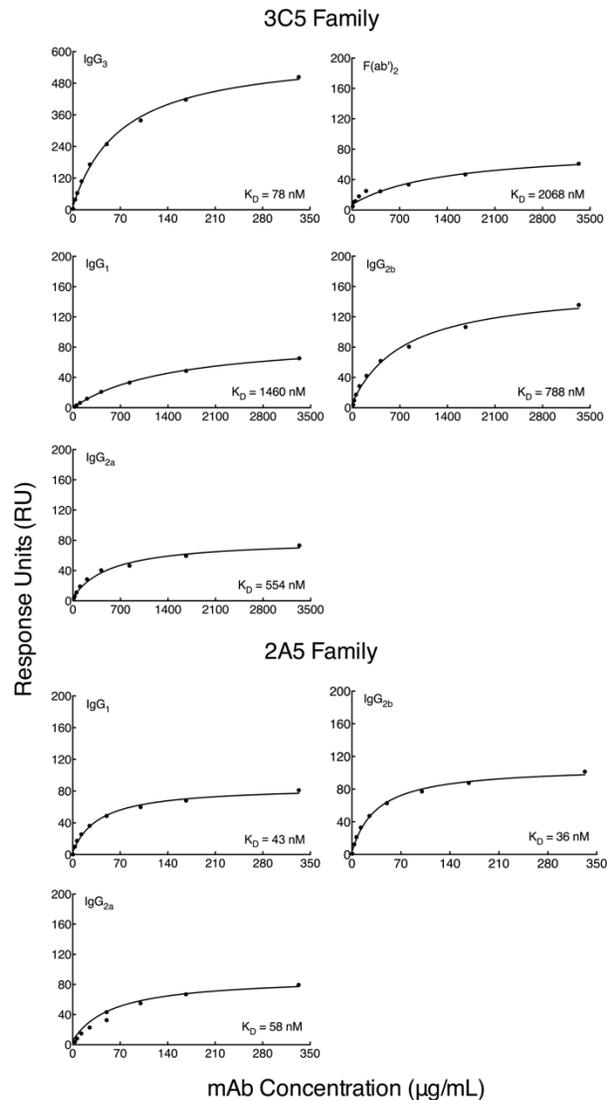
Figure 3. Binding affinity of subclass-switch family mAbs and 3C5 IgG$_3$ F(ab')$_2$ fragments given as a function of response generated by concentration. The steady state model from BIAevaluation software was applied to each graph in Fig 2 to determine the dissociation constant (K$_D$) of each mAb. A smaller K$_D$ corresponds to a higher affinity. Note the magnitude of the response for 3C5 IgG$_3$ compared to all other mAbs, even when affinity is equivalent.
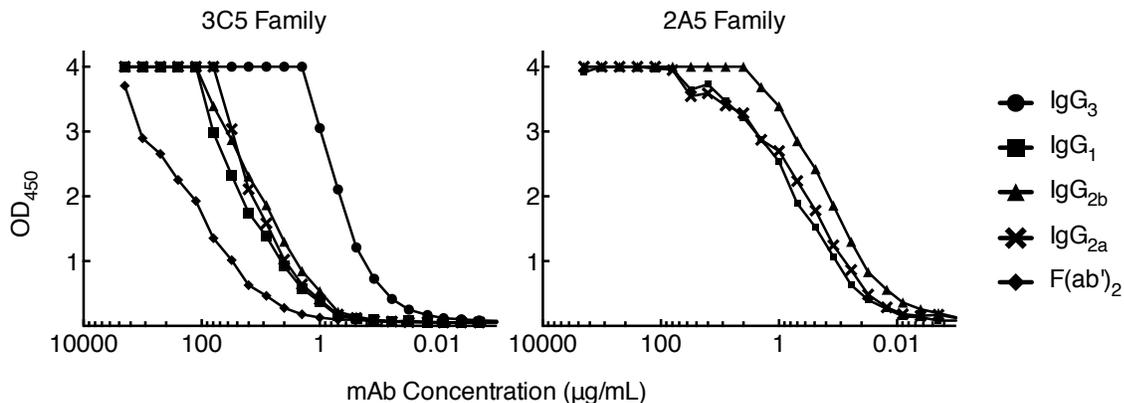
Figure 4. Direct antigen binding ELISA comparing 3C5 IgG_3 and 2A5 IgG_1 binding with subclass with switch family mAbs. CPS was immobilized in the solid phase at 4 μg/mL. 2-fold serial dilutions of mAb or $F(ab')_2$ were added in the fluid phase starting at 2,000 μg/mL and mAb binding was detected with an HRP-conjugated goat anti-mouse kappa chain antibody. There is a significant decrease in binding when altering or removing the IgG_3 Fc region, whereas binding remains constant when subclass-switching the IgG_1 Fc region.
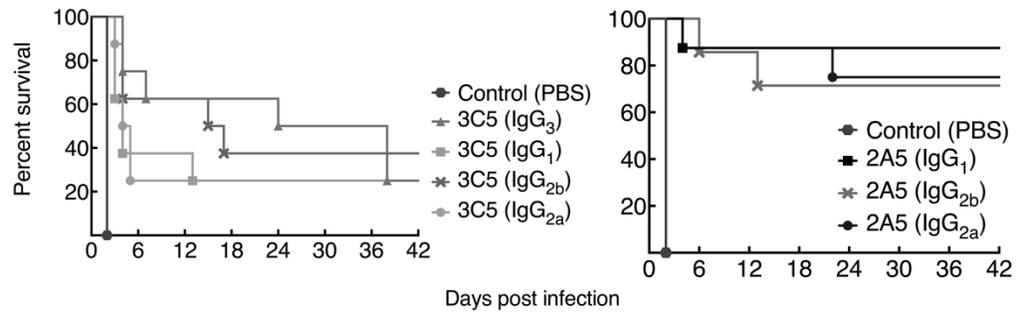
Figure 5. Protection levels afforded by each mAb in mice passively immunized prior to infection with *B. pseudomallei* 1026b. BALB/c mice were administered 1 mg of mAb by the i.p. route; control mice received PBS. After 18 hours, i.n. challenge was performed with 21 LD_{50} of *B. pseudomallei.* Mice were observed daily for 42 days. The *p* values of survival vs. controls are in Table 2.

Figure 6. Weight profiles of passively immunized mice in Fig 5. All infected mice showed reduced activity, a temporary decrease in weight, and moderate illness. Mice immunized with the 3C5 subclass family mAbs were more likely to succumb during later stages of infection, indicated by short time period of diminished clinical symptoms and an increase in weight before a sharp decrease in weight and subsequent death. A ✝ indicates mouse death.

Table 2. Survival and gross pathology of passively immunized mice infected with *B. pseudomallei* 1026b.

mAb	Subclass	Mean time-to-death	Survived (*p* value)[b]	(+) Spleen cfu[c] (*p* value)[d]	Spleen cfu of survivors[e]	Abscess formation[f]
3C5	IgG$_3$	31	2/8 (< 0.01)	7/8 (= 1)	8,0	0/2
	IgG$_1$	4	2/8 (< 0.01)	7/8 (= 1)	22,0	0/2
	IgG$_{2b}$	16	3/8 (< 0.01)	5/8 (= 0.2)	0,0,0	0/3
	IgG$_{2a}$	4.5	1/8 (< 0.01)	7/8 (= 1)	0	0/1
2A5	IgG$_1$	UD	7/8 (< 0.01)	4/8 (= 0.07)	ND,0,0,3,ND,0,0	2/7
	IgG$_{2b}$	UD	5/7 (< 0.01)	5/7 (= 0.2)	0,0,T,7,5	0/6
	IgG$_{2a}$	UD	6/8 (< 0.01)	5/8 (= 0.2)	0,2,368,5,0,0	0/6

[a]Mean time-to-death in days; UD indicates too few deaths to calculate.

[b]*p* value vs. controls determined by Kaplan-Meier survival plots by log-rank (Mantel-Cox) test.

[c]Positive spleen cfu was determined on survivors and assumed to occur In mice that died before study endpoint.

[d]p values vs. controls determined by Fisher's exact test.

[e]Spleen cfu was assessed on survivors only.

 ND indicates an abscess was present, but cfu counts were not determined, T indicates too numerous to count.

[f]Determination of abscess formation on internal organs was performed on survivors only.

References

1. **Shaw BM, Daubenspeck JM, Simmons WL, Dybvig K.** 2013. EPS-I polysaccharide protects Mycoplasma pulmonis from phagocytosis. FEMS Microbiol. Lett. **338:**155-160.

2. **Lemire P, Houde M, Lecours MP, Fittipaldi N, Segura M.** 2012. Role of capsular polysaccharide in Group B Streptococccus interactions with dendritic cells. Microbes Infect **14:**1064-1076.

3. **Melin M, Jarva H, Siira L, Meri S, Käyhty H, Väkeväinen M.** 2009. Streptococcus pneumoniae capsular serotype 19F is more resistant to C3 deposition and less sensitive to opsonophagocytosis than serotype 6B. Infect. Immun. **77:**676-684.

4. **Agarwal S, Vasudhev S, DeOliveira RB, Ram S.** 2014. Inhibition of the classical pathway of complement by meningococcal capsular polysaccharides. J. Immunol. **193:**1855-1863.

5. **Reckseidler-Zenteno SL, DeVinney R, Woods DE.** 2005. The capsular polysaccharide of Burkholderia pseudomallei contributes to survival in serum by reducing complement factor C3b deposition. Infect. Immun. **73:**1106-1115.

6. **Berti F, Campisi E, Toniolo C, Morelli L, Crotti S, Rosini R, Romano MR, Pinto V, Brogioni B, Torricelli G, Janulczyk R, Grandi G, Margarit I.** 2014. Structure of the type IX Group B Streptococcus capsular

polysaccharide and its evolutionary relationship with types V and VII. J. Biol. Chem.

7. **Xie O, Bolgiano B, Gao F, Lockyer K, Swann C, Jones C, Delrieu I, Njanpop-Lafourcade BM, Tamekloe TA, Pollard AJ, Norheim G.** 2012. Characterization of size, structure and purity of serogroup X Neisseria meningitidis polysaccharide, and development of an assay for quantification of human antibodies. Vaccine **30:**5812-5823.

8. **Bruckner V, Kovacs J, Denes G.** 1953. Structure of poly-D-glutamic acid isolated from capsulated strains of B. anthracis. Nature **172:**508.

9. **Heiss C, Burtnick MN, Wang Z, Azadi P, Brett PJ.** 2012. Structural analysis of capsular polysaccharides expressed by Burkholderia mallei and Burkholderia pseudomallei. Carbohydr. Res. **349:**90-94.

10. **Parker DC.** 1993. T cell-dependent B cell activation. Annu. Rev. Immunol. **11:**331-360.

11. **Vos Q, Lees A, Wu ZQ, Snapper CM, Mond JJ.** 2000. B-cell activation by T-cell-independent type 2 antigens as an integral part of the humoral immune response to pathogenic microorganisms. Immunol. Rev. **176:**154-170.

12. **Claesson BA, Trollfors B, Lagergard T, Taranger J, Bryla D, Otterman G, Cramton T, Yang Y, Reimer CB, Robbins JB.** 1988. Clinical and immunologic responses to the capsular polysaccharide of Haemophilus

influenzae type b alone or conjugated to tetanus toxoid in 18- to 23-month-old children. J. Pediatr. **112:**695-702.

13. **Beuvery EC, Miedema F, van Delft R, Haverkamp J.** 1983. Preparation and immunochemical characterization of meningococcal group C polysaccharide-tetanus toxoid conjugates as a new generation of vaccines. Infect. Immun. **40:**39-45.

14. **Burtnick MN, Heiss C, Roberts RA, Schweizer HP, Azadi P, Brett PJ.** 2012. Development of capsular polysaccharide-based glycoconjugates for immunization against melioidosis and glanders. Front Cell Infect Microbiol **2:**108.

15. **Scott MG, Shackelford PG, Briles DE, Nahm MH.** 1988. Human IgG subclasses and their relation to carbohydrate antigen immunocompetence. Diagn. Clin. Immunol. **5:**241-248.

16. **Der Balian GP, Slack J, Clevinger BL, Bazin H, Davie JM.** 1980. Subclass restriction of murine antibodies. III. Antigens that stimulate IgG3 in mice stimulate IgG2c in rats. J. Exp. Med. **152:**209-218.

17. **Perlmutter RM, Hansburg D, Briles DE, Nicolotti RA, Davie JM.** 1978. Subclass restriction of murine anti-carbohydrate antibodies. J. Immunol. **121:**566-572.

18. **Slack J, Der-Balian GP, Nahm M, Davie JM.** 1980. Subclass restriction of murine antibodies. II. The IgG plaque-forming cell response to thymus-

independent type 1 and type 2 antigens in normal mice and mice expressing an X-linked immunodeficiency. J. Exp. Med. **151:**853-862.

19. **Hansburg D, Perlmutter RM, Briles DE, Davie JM.** 1978. Analysis of the diversity of murine antibodies to dextran B1355. III. Idiotypic and spectrotypic correlations. Eur. J. Immunol. **8:**352-359.

20. **Spira G, Bargellesi A, Teillaud JL, Scharff MD.** 1984. The identification of monoclonal class switch variants by sib selection and an ELISA assay. J. Immunol. Methods **74:**307-315.

21. **Hovenden M, Hubbard MA, Aucoin DP, Thorkildson P, Reed DE, Welch WH, Lyons CR, Lovchik JA, Kozel TR.** 2013. IgG subclass and heavy chain domains contribute to binding and protection by mAbs to the poly γ-D-glutamic acid capsular antigen of Bacillus anthracis. PLoS Pathog. **9:**e1003306.

22. **Cooper LJ, Schimenti JC, Glass DD, Greenspan NS.** 1991. H chain C domains influence the strength of binding of IgG for streptococcal group A carbohydrate. J. Immunol. **146:**2659-2663.

23. **Cooper LJ, Robertson D, Granzow R, Greenspan NS.** 1994. Variable domain-identical antibodies exhibit IgG subclass-related differences in affinity and kinetic constants as determined by surface plasmon resonance. Mol. Immunol. **31:**577-584.

24. **Schreiber JR, Cooper LJ, Diehn S, Dahlhauser PA, Tosi MF, Glass DD, Patawaran M, Greenspan NS.** 1993. Variable region-identical

monoclonal antibodies of different IgG subclass directed to Pseudomonas aeruginosa lipopolysaccharide O-specific side chain function differently. J. Infect. Dis. **167:**221-226.

25. **Hubbard MA, Thorkildson P, Kozel TR, AuCoin DP.** 2013. Constant domains influence binding of mouse-human chimeric antibodies to the capsular polypeptide of Bacillus anthracis. Virulence **4:**483-488.

26. **Nuti DE, Crump RB, Dwi Handayani F, Chantratita N, Peacock SJ, Bowen R, Felgner PL, Davies DH, Wu T, Lyons CR, Brett PJ, Burtnick MN, Kozel TR, AuCoin DP.** 2011. Identification of circulating bacterial antigens by in vivo microbial antigen discovery. MBio **2**.

27. **AuCoin DP, Reed DE, Marlenee NL, Bowen RA, Thorkildson P, Judy BM, Torres AG, Kozel TR.** 2012. Polysaccharide specific monoclonal antibodies provide passive protection against intranasal challenge with Burkholderia pseudomallei. PLoS One **7:**e35386.

28. **Kozel TR, Murphy WJ, Brandt S, Blazar BR, Lovchik JA, Thorkildson P, Percival A, Lyons CR.** 2004. mAbs to Bacillus anthracis capsular antigen for immunoprotection in anthrax and detection of antigenemia. Proc. Natl. Acad. Sci. U. S. A. **101:**5042-5047.

29. **Kozel TR, Hermerath CA.** 1988. Benzoquinone activation of Cryptococcus neoformans capsular polysaccharide for construction of an immunoaffinity column. J. Immunol. Methods **107:**53-58.

30. **DeShazer D, Waag DM, Fritz DL, Woods DE.** 2001. Identification of a Burkholderia mallei polysaccharide gene cluster by subtractive hybridization and demonstration that the encoded capsule is an essential virulence determinant. Microb. Pathog. **30:**253-269.

31. **Crisel RM, Baker RS, Dorman DE.** 1975. Capsular polymer of Haemophilus influenzae, type b. I. Structural characterization of the capsular polymer of strain Eagan. J. Biol. Chem. **250:**4926-4930.

32. **DeVoe IW.** 1982. The meningococcus and mechanisms of pathogenicity. Microbiol. Rev. **46:**162-190.

33. **Cherniak R, Valafar H, Morris LC, Valafar F.** 1998. Cryptococcus neoformans chemotyping by quantitative analysis of 1H nuclear magnetic resonance spectra of glucuronoxylomannans with a computer-simulated artificial neural network. Clin. Diagn. Lab. Immunol. **5:**146-159.

34. **Zwartouw HT, Smith H.** 1956. Polyglutamic acid from Bacillus anthracis grown in vivo; structure and aggressin activity. Biochem. J. **63:**437-442.

35. **Wilkinson JF.** 1958. The extracellualr polysaccharides of bacteria. Bacteriol. Rev. **22:**46-73.

36. **Kanaphun P, Thirawattanasuk N, Suputtamongkol Y, Naigowit P, Dance DA, Smith MD, White NJ.** 1993. Serology and carriage of Pseudomonas pseudomallei: a prospective study in 1000 hospitalized children in northeast Thailand. J. Infect. Dis. **167:**230-233.

37. **Feldmann M, Easten A.** 1971. The relationship between antigenic structure and the requirement for thymus-derived cells in the immune response. J. Exp. Med. **134:**103-119.

38. **Jones SM, Ellis JF, Russell P, Griffin KF, Oyston PC.** 2002. Passive protection against Burkholderia pseudomallei infection in mice by monoclonal antibodies against capsular polysaccharide, lipopolysaccharide or proteins. J. Med. Microbiol. **51:**1055-1062.

39. **Zhang S, Feng SH, Li B, Kim HY, Rodriguez J, Tsai S, Lo SC.** 2011. In Vitro and In Vivo studies of monoclonal antibodies with prominent bactericidal activity against Burkholderia pseudomallei and Burkholderia mallei. Clin. Vaccine Immunol. **18:**825-834.

40. **Bottex C, Gauthier YP, Hagen RM, Finke EJ, Splettstosser WD, Thibault FM, Neubauer H, Vidal DR.** 2005. Attempted passive prophylaxis with a monoclonal anti-Burkholderia pseudomallei exopolysaccharide antibody in a murine model of melioidosis. Immunopharmacol. Immunotoxicol. **27:**565-583.

41. **Nelson M, Prior JL, Lever MS, Jones HE, Atkins TP, Titball RW.** 2004. Evaluation of lipopolysaccharide and capsular polysaccharide as subunit vaccines against experimental melioidosis. J. Med. Microbiol. **53:**1177-1182.

42. **Brett PJ, Woods DE.** 1996. Structural and immunological characterization of Burkholderia pseudomallei O-polysaccharide-flagellin protein conjugates. Infect. Immun. **64:**2824-2828.

43. **Bryan LE, Wong S, Woods DE, Dance DA, Chaowagul W.** 1994. Passive protection of diabetic rats with antisera specific for the polysaccharide portion of the lipopolysaccharide isolated from Pseudomonas pseudomallei. Can. J. Infect. Dis. **5:**170-178.

44. **Tudor D, Yu H, Maupetit J, Drillet AS, Bouceba T, Schwartz-Cornil I, Lopalco L, Tuffery P, Bomsel M.** 2012. Isotype modulates epitope specificity, affinity, and antiviral activities of anti-HIV-1 human broadly neutralizing 2F5 antibody. Proc. Natl. Acad. Sci. U. S. A. **109:**12680-12685.

45. **Torres M, Fernandez-Fuentes N, Fiser A, Casadevall A.** 2007. The immunoglobulin heavy chain constant region affects kinetic and thermodynamic parameters of antibody variable region interactions with antigen. J. Biol. Chem. **282:**13917-13927.

46. **Wang TT, Lucas AH.** 2004. The capsule of Bacillus anthracis behaves as a thymus-independent type 2 antigen. Infect. Immun. **72:**5460-5463.

47. **Greenspan NS, Dacek DA, Cooper LJ.** 1989. Cooperative binding of two antibodies to independent antigens by an Fc-dependent mechanism. FASEB J. **3:**2203-2207.

48. **Kozel TR, Thorkildson P, Brandt S, Welch WH, Lovchik JA, AuCoin DP, Vilai J, Lyons CR.** 2007. Protective and immunochemical activities of monoclonal antibodies reactive with the Bacillus anthracis polypeptide capsule. Infect. Immun. **75:**152-163.

49. **Chen Z, Schneerson R, Lovchik J, Lyons CR, Zhao H, Dai Z, Kubler-Kielb J, Leppla SH, Purcell RH.** 2011. Pre- and postexposure protection against virulent anthrax infection in mice by humanized monoclonal antibodies to Bacillus anthracis capsule. Proc. Natl. Acad. Sci. U. S. A. **108:**739-744.

50. **Mukherjee J, Scharff MD, Casadevall A.** 1992. Protective murine monoclonal antibodies to Cryptococcus neoformans. Infect. Immun. **60:**4534-4541.

51. **Yuan R, Casadevall A, Spira G, Scharff MD.** 1995. Isotype switching from IgG3 to IgG1 converts a nonprotective murine antibody to Cryptococcus neoformans into a protective antibody. J. Immunol. **154:**1810-1816.

52. **Yuan RR, Spira G, Oh J, Paizi M, Casadevall A, Scharff MD.** 1998. Isotype switching increases efficacy of antibody protection against Cryptococcus neoformans infection in mice. Infect. Immun. **66:**1057-1062.

53. **Sarkar-Tyson M, Titball RW.** 2010. Progress toward development of vaccines against melioidosis: A review. Clin. Ther. **32:**1437-1445.

54. **Scott AE, Burtnick MN, Stokes MG, Whelan AO, Williamson ED, Atkins TP, Prior JL, Brett PJ.** 2014. Burkholderia pseudomallei capsular polysaccharide conjugates provide protection against acute melioidosis. Infect. Immun. **82:**3206-3213.

Chapter 2

Development of a mAb library targeting the capsular polysaccharide of

***Burkholderia pseudomallei* for the diagnosis of melioidosis**

Michael J. Dillon, Rachael A. Loban, Dana E. Reed, Peter Thorkildson, Raymond

Houghton, Syamal Raychaudhuri, Jean Chen, Paul J. Brett, Mary N. Burtnick,

and David P. AuCoin*

Department of Microbiology and Immunology, University of Nevada School of

Medicine, Reno, Nevada, 89557

Department of Cellular and Molecular Biology, University of Nevada School of

Medicine, Reno, Nevada, 89557

*Corresponding author. Mailing address: Department of Microbiology and

Immunology/320, University of Nevada School of Medicine, 1667 North Virginia

Street, Reno, NV 89557.

Phone: (775) 784-4128. Fax: (775) 327-2332. E-mail:

daucoin@medicine.nevada.edu

Abstract

Burkholderia pseudomallei, the causative agent of melioidosis, causes significant morbidity and mortality across Southeast Asia. The bacterium's high virulence comes in part from its capsule; it is encapsulated with a high molecular weight capsular polysaccharide (CPS) that inhibits phagocytosis, inhibits complement deposition, and is essential for virulence. Previously, our laboratory determined that low levels of CPS are shed into patient sera and urine and identified CPS as a possible diagnostic marker for *B. pseudomallei* infection. In a preliminary study, we produced a CPS-specific IgG_3 monoclonal antibody (mAb), 3C5, and successfully incorporated it into a prototype Active Melioidosis Detect™ Lateral Flow Immunoassay (AMD LFI) through a collaboration with InBios International, Inc. While successful, the prototype had background issues attributed to IgG_3 self-association that would potentially produce false positive results. This led us to pursue the development of additional antibodies of alternate IgG subclasses. We have isolated an IgG_1 mAb, 4C4, which has reduced background reactivity compared to mAb 3C5. Additionally, this new mAb displays a high affinity for CPS and can detect lower concentrations of CPS in solution. Use of the improved mAb may allow for a LFI with improved clinical sensitivity. An updated LFI incorporating mAb 4C4 has been produced as a potential rapid diagnostic for melioidosis.

Introduction

Burkholderia pseudomallei is a soil-dwelling, gram-negative bacillus. It is the causative agent of melioidosis, a highly prevalent disease in Southeast Asia and Northern Australia. *B. pseudomallei* infects roughly 21 out of every 100,000 people in Northeast Thailand each year, and of those infected, only about 50% survive the infection (1). Survival rates are higher in Australia, where intensive therapy is more readily available; here, 80% of all melioidosis patients survive (2). Even so, survival does not guarantee immunity to repeat infections. Roughly 20% of all melioidosis survivors will suffer a relapse infection and contract the disease a second (or third) time (3). While there have been several melioidosis vaccine studies in animals, none of them have been effective at eliciting sterilizing immunity (4).

Melioidosis is a febrile illness that is incredibly difficult to diagnose because it mimics the symptoms of so many other diseases. Infected patients may present flu-like symptoms, pneumonia, and bacteremia (5). There is usually a 7-10 day incubation period in infected individuals; however, some cases can take several years to manifest (6, 7). Rapid diagnosis of melioidosis is critical; *B. pseudomallei* is resistant to the most commonly prescribed antibiotics and any delay in treatment is correlated with higher patient relapse rates (8). Currently, bacterial culture is the gold

standard for diagnosis of melioidosis, however, it may take 7-10 days to confirm infection via culture, and it is only about 60% accurate (9).

B. pseudomallei produces a high molecular weight capsular polysaccharide (CPS) comprised of an unbranched homopolymer of *manno*heptopyranose residues (10). The CPS is responsible for *B. pseudomallei* persistence in the blood by preventing the deposition of complement factor C3b and inhibiting phagocytosis (11). As such, it is essential for virulence (12). Melioidosis survival rates are correlated with high antibody titers against CPS (13); antibodies to capsules can act as an intermediary by assisting complement deposition and promoting phagocytosis (14). Unfortunately, capsules are generally T-cell independent type-2 (TI-2) antigens (15). They activate B-cells by multivalent cross-linking of antigen receptors, eliciting a weak, non-persistent humoral immune response (16).

Our laboratory previously developed a diagnostic biomarker discovery platform, *in vivo* microbial antigen discovery (InMAD) (17). InMAD studies showed that *B. pseudomallei* CPS is shed into patient samples, and we identified the CPS as a potential biomarker for the diagnosis of melioidosis (17). We generated a murine IgG_3 monoclonal antibody (mAb) and developed a prototype Active Melioidosis Detect™ Lateral Flow Immunoassay (AMD LFI). The prototype AMD LFI is able to detect CPS shed into patient serum and urine samples at a limit of 0.2

ng/mL to diagnose melioidosis in 15 minutes or less (18). While very successful, the prototype suffers from background issues attributed to IgG_3 self-association. IgG_3 is the predominate response to polysaccharides in mice (19-21), and research has shown that this antibody subclass can bind cooperatively to multivalent antigens (22-24).

The goal of the present study was to improve upon a prototype AMD LFI by generating a library of high affinity mAbs against the CPS of *B. pseudomallei* in order to eliminate background issues and increase sensitivity. Our results demonstrate that mAb 4C4 is an ideal candidate for an updated AMD LFI.

Materials and Methods

Immunization of mice and production of mAbs. Generation of mAb 3C5 has been described (25). MAbs were produced using CPS conjugated to bovine serum albumin (BSA) (26). BALB/c mice were immunized via intraperitoneal (i.p.) injections with 5 μg of CPS-BSA every two weeks for six weeks total. An ELISA was used to determine antibody titers to *B. pseudomallei* CPS (see below). A final boost with purified CPS was administered three days prior to splenectomy. Hybridoma cells were produced as previously described (27). Western blot analysis was done to identify hybridoma cell lines that were producing mAbs reactive with purified CPS. Cell lines were grown in Integra CL 1000 culture flasks (Integra Biosciences) with RPMI media containing 50 μM 2-mercaptoethanol, 20 mM HEPES, 1 mM sodium pyruvate, and 15% FBS (low IgG). Antibodies were purified by affinity chromatography over a protein A column.

Western blot. 1 μL of a 10x concentrated *B. pseudomallei* 1026b lysate (Dr. Richard Bowen, Colorado State University), 1.1 x 10^5 cfu of *B. mallei* China 7 (BEI), 8 x 10^6 cfu of *B. thailandensis* E264 (BEI), or 0.5 μg purified CPS were incubated with 1 volume of proteinase K at 3.3 mg/mL for 1 hr at 60 °C. Next, samples were separated by sodium dodecyl sulfate-12% polyacrylamide gel electrophoresis (SDS PAGE) (BioRad) at 160 V for 1 hr, followed by transfer to a nitrocellulose membrane (BioRad) via a

TransBlot Turbo (BioRad). Membranes were blocked in TBS+0.1% Tween 20, 5% milk overnight (blocking solution) at 4 °C. Membranes were then probed with mAbs diluted at 0.1 μg/m in blocking solution while rocking at room temperature for 1 hr. Membranes were washed for 15 min, 3 separate times, with TBS+0.1% Tween 20 and mAb binding was detected with peroxidase-conjugated goat anti-mouse kappa chain antibody (Southern Biotech) diluted 1:10,000 in blocking solution and incubated for 30 min at room temperature. Membranes were washed 3 additional times and binding was detected with SuperSignal West Femto Chemiluminescent Substrate (Pierce). Binding was visualized with Chemidoc Instruments (BioRad).

Surface plasmon resonance. Binding affinity was determined using surface plasmon resonance (SPR) with a BIAcore X100 (GE Healthcare). Purified CPS was benzoquinone activated and conjugated to biotin as previously described (29), and immobilized onto a streptavidin (SA) sensor chip at 30 response units (RU). A second flow cell was unmodified and used for reference subtractions. Affinity was evaluated with mAbs diluted in HBS-EP+ running buffer (10 mM HEPES, 150 mM NaCl, 3 mM EDTA, and 0.05% surfactant P20) at a range of 0-333 nM. 2-fold serial dilutions of mAb were injected over the immobilized CPS at 30 μL/min for 60 s, followed by 120 s of passive dissociation. The sensor chip surface was

regenerated between each concentration with 10 mM HCl, pH 1.5. Affinity was determined using BIAevaluation software (GE Healthcare).

Direct antigen enzyme-linked immunosorbent assay (ELISA). Polystyrene plates (Thermo Scientific) were coated for 90 min at 37°C with 0.005% (w/v) Poly-L-Lysine (Sigma) diluted in PBS. Plates were washed with PBS and incubated overnight with 4 μg/mL of purified CPS (26). Next, plates were washed with PBS+0.05% Tween 20 and blocked with PBS+0.05% Tween 20, 5% milk (blocking solution) at 37 °C for 90 min. MAbs (or mouse sera) were serial diluted across the wells in blocking solution, starting at 2000 μg/mL, and the plates were incubated at 37 °C for 90 min. MAb binding was detected with peroxidase-conjugated goat anti-mouse kappa chain antibody (or peroxidase-conjugated goat anti-mouse IgG antibody) (Southern Biotech) diluted in blocking solution at 1:10,000 and incubated for 90 min, followed by TMB peroxidase substrate (KPL) for 30 min. The enzymatic reaction was stopped by adding 100 μL of 5% o-phosphoric acid to each well and the optical density was determined by measuring absorbance at 450 nm. Each experiment was completed in duplicate. To calculate the antibody concentration that induces a response halfway between baseline and maximum (EC_{50} value), a four-parameter logistics curve fit was applied using Sigma Plot 11.0 (Systat Software Inc.)

Antigen capture enzyme-linked immunosorbent assay (ELISA).
Antigen capture ELISA was performed as previously described (17). In
summary, antibodies were conjugated to horseradish peroxidase (HRP)
with Pierce EZ-Link Plus Activated Peroxidase (Thermo Scientific)
following the manufacturer's protocol. Polystyrene plates (Thermo
Scientific) were coated overnight at room temperature with 2 μg/mL of
unlabeled mAb. Plates were washed with PBS+0.05% Tween 20 and
blocked with PBS+0.05% Tween 20, 5% milk (blocking solution) at 37 °C
for 90 minutes. Purified CPS was serially diluted in blocking solution and
incubated at 37 °C for 90 minutes. HRP-conjugated mAbs were diluted in
blocking solution and added to wells at a final concentration of 4 μg/mL or
at a 1:10,000 dilution and incubated at room temperature for 90 minutes.
MAb binding was detected with tetramethylbenzidine (TMB) peroxidase
substrate (KPL) for 30 minutes. The enzymatic reaction was stopped with
5% *o*-phosphoric acid and the optical density was determined by
measuring absorbance at 450 nm. Each experiment was completed in
duplicate. To calculate limit of detection (LOD) values, data was
normalized in SoftMax Pro at an OD_{450} value of 0.3 (Molecular Devices).

AMD LFI construction. AMD LFIs were prepared as previously described
(18). In short, mAbs were sprayed onto the test line on a nitrocellulose
membrane. Goat anti-chicken IgY was sprayed onto the same membrane
for the control line. Each mAb, along with chicken IgY (for the control line)

was conjugated to 40 nm gold nanoparticles and dried in the conjugate pad. The sample pad, conjugate pad, and membrane were all assembled in an overlapping fashion atop a plastic back.

AMD LFI sample preparation and testing. Five-fold serial dilutions of purified CPS (25-0.008 ng/mL) were made in 150 μL of chase buffer, human urine, or human serum and added directly to the sample pad. Images were taken after 15 minutes. The AMD LFI was shown to 5 independent parties and the limit of detection was determined as the lowest value that all 5 people indicated seeing a red test line.

Bacterial colonies were tested as previously described (18). Briefly, bacteria were streaked for isolation on brain-heart infusion (BHI) agar and incubated at 37 °C overnight. An entire colony was suspended in 2 drops of lysis buffer and added directly to the sample pad, followed by 3 drops of chase buffer. Images were taken after 15 minutes.

Ethics statement. All studies were carried out in accordance with the recommendations in the Guide for the Care and Use of Laboratory Animals of the National Institutes of Health. The Animal Care and Use Committees at the University of Nevada, Reno (Protocol A07/08-16) approved all protocols.

Results

MAb 3C5 (IgG$_3$) was generated as previously described (25). IgG$_1$ mAbs were generated from BALB/c mice immunized with purified CPS conjugated to BSA (26). Splenocytes from immunized mice were fused with myeloma cells to generate mAb-secreting hybridomas. Total mRNA was isolated from each hybridoma cell line and used for cDNA synthesis and PCR amplification. PCR products were ligated into pGEM-T and sequenced to ensure that the variable region of each mAb in the library is unique.

All 8 mAbs were verified to bind to CPS via Western Blot; CPS is a produces a very characteristic smear at high molecular weights via Western Blot (10). All mAbs bound at similar concentrations to a Proteinase K-resistant high molecular weight antigen found in *B. pseudomallei* and *Burkholderia mallei*. MAbs also bound to purified CPS. MAbs did not bind to *Burkholderia thailandensis* lysate, which lacks CPS (Fig 1) (30).

In order to elucidate the binding characteristics of each mAb in the library, the affinities were determined with SPR with a BIAcore X100. Purified CPS was conjugated to biotin (29) and immobilized on a streptavidin-coated sensor chip. Total immobilization of CPS was 30 *RU*. A titratable increase in *RU* was observed following a 60 second pulse of each mAb concentration (0-333 nM) (Fig 2). The steady state model from

the BIAevaluation software was applied to determine the dissociation constant (K_D) of each mAb (Fig 3). The calculated binding affinity of each mAb is in Table 1. MAbs 2A5, 1A2, and 4C4 all bound to CPS more strongly than our original mAb 3C5, however, mAb 3C5 exhibited a much greater response. 4C4 has the greatest binding affinity in the library with an observed K_D of 12 nM, whereas mAb 3B4 had the lowest calculated K_D at 139 nM. MAbs 1D3, 2B3, and 1D4 had K_D values too low to accurately assess.

Next, a direct antigen ELISA was performed to further assess the binding characteristics of mAbs 2A5, 1A2, 4C4 and 3B4 when compared to our original mAb 3C5 (Fig 4). Purified CPS was bound in the solid phase at 4 μg/mL and 2-fold serial dilutions of the mAbs were diluted in the fluid phase starting at 2,000 μg/mL. Each line on the plot represents a different mAb. These plots were used to calculate the half maximal effective concentration value (EC_{50}), which is the antibody concentration that generates a response halfway between the baseline and maximum; smaller values correlate with a higher potency (Table 1). Similar to the affinity data, mAb 4C4 had the lowest EC_{50} value, at 0.16 μg/mL while 3B4 had the highest EC_{50} value at 22 μg/mL.

Additionally, sandwich ELISAs were performed in order to determine how the mAbs interact with each other and with CPS in the capture and detection phases (Fig 5). Antibody was bound in the solid

phase at 2 μg/mL and 2-fold serial dilutions of CPS were diluted in the solid phase starting at 640 ng/mL. Next, each mAb was conjugated to HRP and diluted in the fluid phase at 4 μg/mL. Each line of the plot represents a different mAb; the same mAb was used for both capture and detection. These plots were used to calculate the limit of detection (LOD) of each mAb combination in order to determine the least amount of CPS required for a signal; a lower LOD means we could theoretically diagnose *B. pseudomallei* infection earlier in infected patients (Table 1). Because of the high levels of background with mAb 3C5, data had to be normalized to calculate the LOD. The LOD was considered to be twice the background levels, or an OD_{450} signal of 0.3. MAb 4C4 in the capture and detection phases showed the lowest LOD at 0.25 ng/mL, followed by our original mAb 3C5 at 0.36 ng/mL. Interestingly, mAbs 2A5 and 1A2 showed a higher calculated LODs than mAb 3C5, at 1.56 and 0.72 ng/mL respectively, even though they had higher affinities. MAb 3B4 has a calculated LOD at 0.70 ng/mL, despite having the lowest affinity of the set. Additional ELISAs were performed with different combinations of mAbs in the capture and detection phases; even still, mAb 4C4 in both the capture and detect phases produced the lowest limit of detection overall (data not shown).

Sample LFIs for each mAb were constructed as previously described to assess how the new mAbs perform in the LFI format (18).

Different combinations of mAbs in the capture (control line) and detection (gold conjugated) phases were assembled and the limit of detection was assayed for each combination (data not shown). The limit of detection was defined as the lowest concentration at which 5 independent parties verified seeing a positive line. MAb 4C4 applied to both the capture and detection phases showed the lowest limit of detection at 0.04 ng/mL, a 5-fold greater limit of detection when compared to the original 3C5 AMD LFI prototype (Fig 6). Human serum and urine samples were spiked with purified CPS in order to verify that human samples would not interfere with the updated AMD LFI.

The updated LFIA was tested against multiple bacteria commonly seen in the soil to verify it would not cross-react and generate false positive results (Table 2). Nine distinct *Burkholderia cepacia* complex (BCC) bacteria were tested. BCC bacteria are soil-dwelling bacteria that are important human pathogens, however, they generally only infect patients with underlying lung disease, such as cystic fibrosis (31). The updated AMD LFI did not react with 8 of the samples, but did interact weakly with *B. stabilis,* which produces minimal CPS (12). Additionally, the AMD LFI did not react with 9 common gram-positive bacteria or 5 common gram-negative bacteria.

Next, the AMD LFI was also tested against 41 unique strains of *B. pseudomallei* and 3 unique strains of *B. mallei* to ensure it would detect a

broad range of infectious strains (Table 2). The AMD LFI was reactive with

40/41 strains of *B. pseudomallei* and all 3 strains of *B. mallei*, but not *B. thailandensis* (which does not produce a capsule) (30).

Finally, the AMD LFI was tested against 20 unique human serum and urine samples to verify it would not react with individuals not infected with *B. pseudomallei*. The AMD LFI was negative for all of these samples.

Discussion

LFIs are becoming increasingly popular and are used to diagnose several diseases, including HIV infection, malaria, coronary artery disease, avian influenza, and community-acquired pneumonia (32, 33). They are inexpensive, user-friendly, and very rapid. LFIs require minimum patient sample for testing and can accommodate a variety of sample types, including saliva, urine, serum, and pus. They are sensitive, with limits of detection comparable to other diagnostic methods and can be read without any equipment (18, 33). This makes them ideal in both resource poor and point-of-care settings where high costs are prohibitive and access to training is limited.

The current diagnostic methods available for *B. pseudomallei* infection suffer from low sensitivity and require expensive equipment, among other drawbacks. For example, immunofluorescence assays (IFA) (34) and polymerase chain reactions (PCR) (35) require equipment and facilities that are not readily available in Northeast Thailand. This lead to the development of indirect hemagglutination assays (IHA) (36) and immunochromogenic cassette tests (ICT) (37) as inexpensive alternatives for rural areas. However, much of the population in endemic areas is seropositive for *B. pseudomallei*, making the presence of antibodies in blood an unreliable diagnostic marker (38).

The AMD LFI avoids this problem by detecting *B. pseudomallei* CPS directly, an antigen that is only found during active infection. Additionally, CPS is a necessary virulence factor; mutations that prevent the biosynthesis of CPS greatly attenuate the bacteria (39, 40). The original prototype AMD LFI was constructed with a murine IgG_3 and was highly successful; it could detect CPS levels as low as 0.2 ng/mL (18). However, it had levels of background that could be misinterpreted for a positive result. This was attributed to self-aggregation phenomena seen in murine IgG_3 antibodies (22-24), thus, we sought to improve the AMD LFI by developing and screening a library of anti-CPS mAbs of different isotypes and subclasses. During the screening process, an IgG_1 mAb, 4C4, had a higher affinity, lower EC_{50} value, and lower limit of detection when compared to the other mAbs in the library, including the original mAb 3C5. As such, mAb 4C4 was used to construct an updated AMD LFI.

Importantly, the updated AMD LFI resolves the background issues seen in our prototype. Additionally, it can detect 5-fold lower levels of CPS than our original prototype, meaning that can possibly be diagnose *B. pseudomallei* infection much earlier than before. It was reactive with 41 out of 42 strains of *B. pseudomallei,* 3 out of 3 strains of *B. mallei* and only reacted very weakly with 1 near neighbor strain of bacteria tested. The cross-reactive near neighbor was *B. stabilis*, which contains the CPS

operon and produces the same capsule, albeit in significantly smaller quantities (12).

The results from this study suggest that non-IgG_3 murine mAbs are ideal for the LFI format and immunization strategies should focus on eliciting a strong IgG_1 immune response. Isolating a high affinity IgG_3 and producing an IgG_1 by subclass switch does not seem like an acceptable alternative; when mAb 3C5 was subclass-switched to an IgG_1, the affinity dropped significantly and the new variant performed very poorly by ELISA (Chapter 1). Thus, immunization strategies should focus on eliciting an alternative immune response. Furthermore, IgM mAbs seem to be poor candidates. We isolated two IgM mAbs and both reacted with CPS very poorly in vitro. This was not unexpected, as IgM antibodies are typically rapidly generated, low-affinity first responders that have not had the opportunity to affinity mature (41).

The updated AMD LFI incorporating mAb 4C4 is currently being tested at various sites across the globe in both clinical and environmental settings. It is currently undergoing a 24 Month Diagnostic Challenge with the Defense Threat Reduction Agency (DTRA) where it is being tested for sensitivity and stability at the Navy Research Laboratory (NRL). Future directions include optimizing the testing procedure for patient samples and improving the limit of detection with europium-based assays.

Acknowledgements

Table 1. Summary of antibodies generated for this study.

mAb	IgG Subclass	K_a ([μM-s]$^{-1}$)[a]	K_d (s^{-1})[b]	K_D (nM)[c]	EC_{50} (μg/mL)	LOD (ng/mL)
3C5	IgG$_3$	0.28	0.0011	73	0.9±0.03	0.36
4C4	IgG$_1$	0.0025	0.0024	1,460	0.16±0.01	0.25
2A5	IgG$_1$	1.8	0.0024	790	0.36±0.02	1.56
1A2	IgG$_1$	0.0009	0.0041	550	0.51±0.03	0.72
3B4	IgG$_1$	0.0002	0.0059	2,100	22±1.4	0.70
1D3	IgG$_1$	-	-	-	-	-
2B3	IgM	-	-	-	-	-
1D4	IgM	-	-	-	-	-

[a]Association rate constant   [b]Dissociation rate constant   [c]Dissociation constant
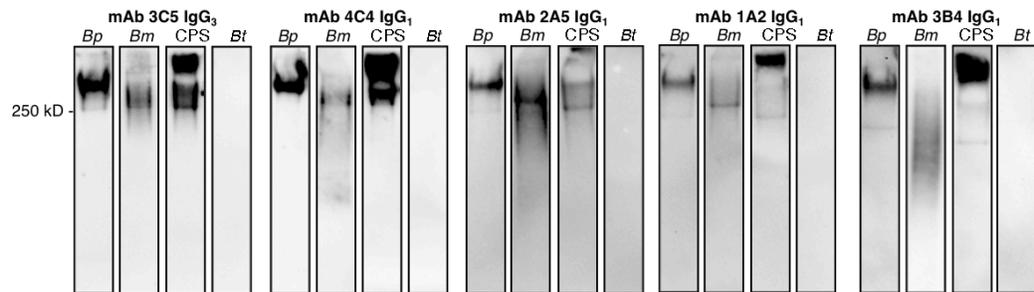
Figure 1. *B. pseudomallei* (*Bp*) 1026b, *B. mallei* (*Bm*) China 7, purified CPS, or *B. thailandensis* (*Bt*) E264 were incubated with proteinase-K, separated by SDS PAGE, and subsequently transferred to a nitrocellulose membrane. Membranes were probed with 0.5 μg mAb and binding was detected with an HRP-conjugated goat anti-mouse kappa chain antibody. All mAbs bind to a high molecular weight, proteinase-K resistant antigen found in *B. pseudomallei*, *B. mallei*, and purified CPS. MAbs do not interact with *B. thailandensis*, which lacks CPS.
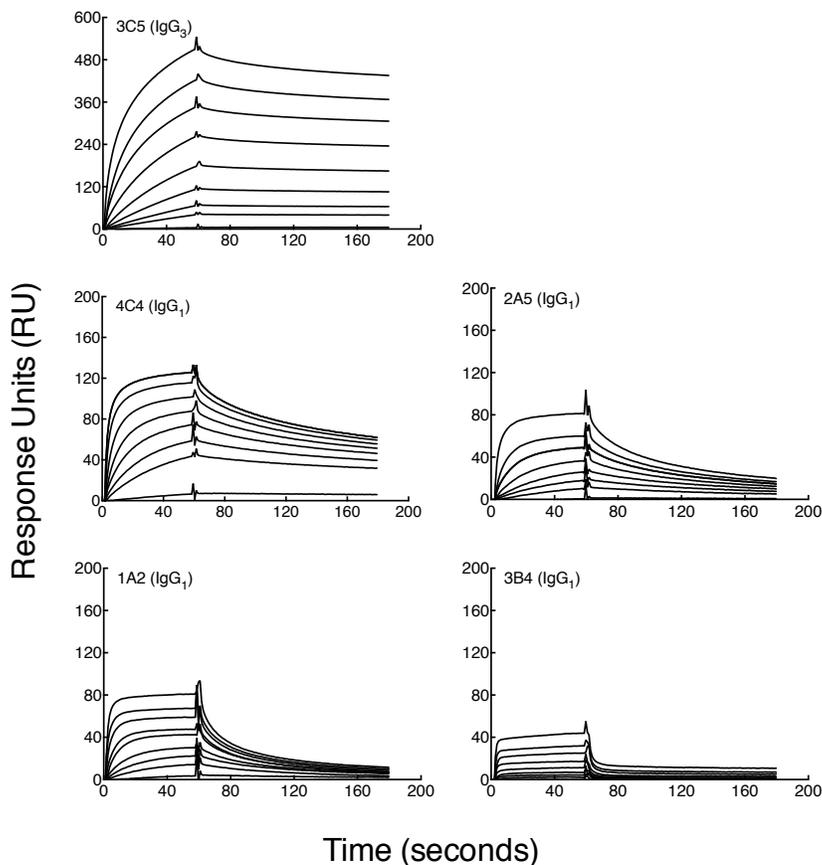

Figure 2. Binding specificity of mAbs given as a function of response generated over time. A BIAcore X100 instrument was used to determine the affinity of each mAb for CPS. Purified CPS was conjugated to biotin and immobilized on a SA sensor chip. MAb binding was analyzed by injecting eight samples (2-fold serial dilutions (0-333 nM) for 60 s, followed by 120 s of passive dissociation. Note the magnitude of the response for 3C5 IgG_3 compared to all other mAbs.
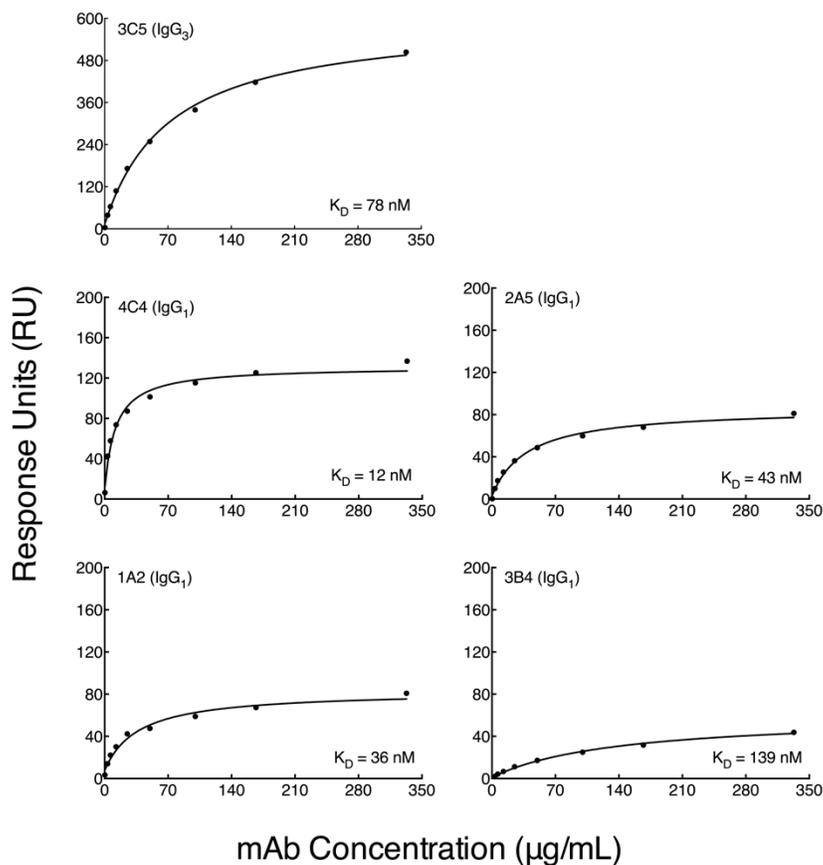
Figure 3. Binding affinity of subclass-switch family mAbs and 3C5 IgG$_3$ F(ab')$_2$ fragments given as a function of response vs. mAb concentration. The steady state model from BIAevaluation software was applied to each graph in Fig 2 to determine the dissociation constant (K$_D$) of each mAb. A smaller K$_D$ corresponds to a higher affinity. Note the magnitude of the response for 3C5 IgG$_3$ compared to all other mAbs, even the resultant binding affinity is equivalent.
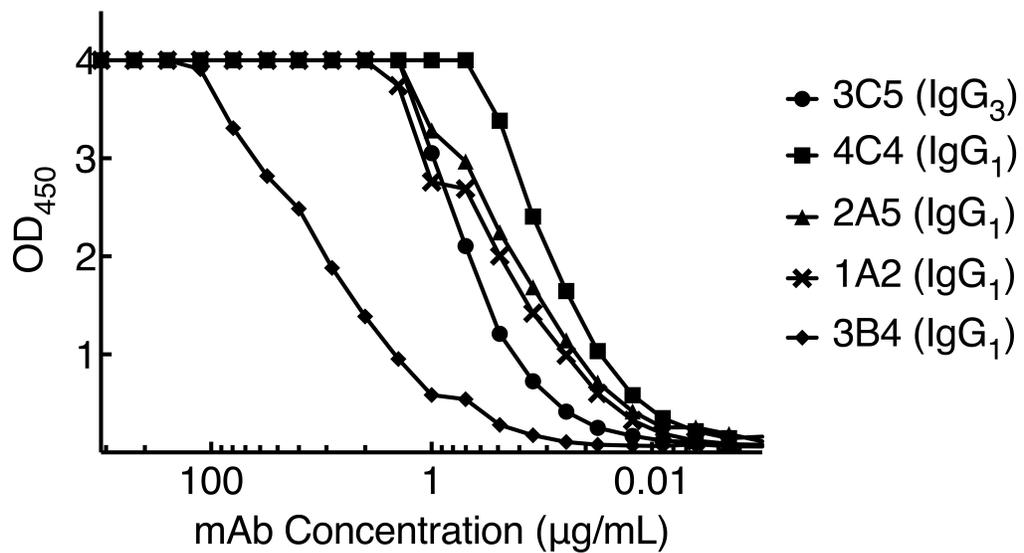
Figure 4. Direct antigen binding ELISA comparing binding of all mAbs. CPS was immobilized in the solid phase at 4 μg/mL. 2-fold serial dilutions of mAb were added in the fluid phase starting at 2,000 μg/mL and mAb binding was detected with an HRP-conjugated goat anti-mouse kappa chain antibody. MAb 4C4 has the lowest EC_{50} value (0.16 ng/mL).

Figure 5. Sandwich ELISA comparing CPS detection capabilities of various mAbs. Purified mAb was immobilized in the solid phase at 2 µg/mL. 2-fold serial dilutions of purified CPS were added in the fluid phase starting at 640 ng/mL. HRP conjugated mAb was used in the detection phase. MAb 4C4 demonstrated the lowest limit of detection (0.25 ng/mL). Note the high levels of background generated by mAb 3C5, possibly due to IgG_3 self-aggregation.

(A) Purified CPS (ng/mL) on 3C5-3C5 Prototype

(B) Purified CPS (ng/mL) on updated 4C4-4C4

Figure 6. LOD comparison of the original 3C5-3C5 prototype with the updated 4C4-4C4 AMD LFI. 5-fold dilutions of purified CPS were diluted in chase buffer starting at 25 ng/mL and applied to the sample pad of the (A) original 3C5-3C5 or (B) new 4C4-4C4 LFI. Results were imaged after 15 minutes. The LOD was the lowest concentration at which 5 independent parties verified seeing a positive line. The updated 4C4-4C4 AMD LFI has a 5-fold greater sensitivity than the original 3C5-3C5 prototype when evaluated in this manner.

Table 2. 4C4-4C4 LFI analytical reactivity and specificity.

Bacterial isolate	Strain designation	Lateral flow result
Burkholderia cepacia	PC783	Negative (-)
Burkholderia cenocepacia	HI2718	Negative (-)
Burkholderia vietnamensis	PC259	Negative (-)
Burkholderia multivorans	HI2229	Negative (-)
Burkholderia anthina	AU1293	Negative (-)
Burkholderia ambifaria	HI2464	Negative (-)
Burkholderia dolosa	FTU0645	Negative (-)
Burkholderia pyrocinia	BCII	Negative (-)
Burkholderia stabilis	HI2210	Weakly positive (+)
Burkholderia stabilis	ATCC LMG 14294	Weakly positive (+)
Burkholderia thailandensis	E264	Negative (-)
Streptococcus viridans	—	Negative (-)
Streptococcus pyogenes	—	Negative (-)
Streptococcus agalactiae	—	Negative (-)
Streptococcus bovis	—	Negative (-)
Streptococcus faecalis	—	Negative (-)
Staphylococcus xylosus	—	Negative (-)
Staphylococcus epidermidis	—	Negative (-)
Staphylococcus aureus	—	Negative (-)
Staphylococcus saprophyticus	—	Negative (-)
Citrobacter freundii	—	Negative (-)
Pseudomonas aeruginosa	—	Negative (-)
Enterobacter aerogenes	—	Negative (-)
Proteus vulgaris	—	Negative (-)
Escherichia coli	—	Negative (-)
Klebsiella pneumoniae	—	Negative (-)

Table 2. Continued.

Bacterial isolate	Strain name/DASH #	Lateral flow result
Burkholderia pseudomallei	1026b	Positive (+)
Burkholderia pseudomallei	Bp82	Positive (+)
Burkholderia pseudomallei	Bp0029	Positive (+)
Burkholderia pseudomallei	Bp0033	Positive (+)
Burkholderia pseudomallei	Bp0034	Positive (+)
Burkholderia pseudomallei	Bp0035	Positive (+)
Burkholderia pseudomallei	Bp0049	Positive (+)
Burkholderia pseudomallei	Bp0056	Positive (+)
Burkholderia pseudomallei	Bp0065	Positive (+)
Burkholderia pseudomallei	Bp0071	Negative (-)
Burkholderia pseudomallei	Bp0072	Positive (+)
Burkholderia pseudomallei	Bp0082	Positive (+)
Burkholderia pseudomallei	Bp0084	Positive (+)
Burkholderia pseudomallei	Bp0096	Positive (+)
Burkholderia pseudomallei	Bp0097	Positive (+)
Burkholderia pseudomallei	Bp0098	Positive (+)
Burkholderia pseudomallei	Bp0099	Positive (+)
Burkholderia pseudomallei	Bp0101	Positive (+)
Burkholderia pseudomallei	Bp0114	Positive (+)
Burkholderia pseudomallei	Bp0115	Positive (+)
Burkholderia pseudomallei	Bp0121	Positive (+)
Burkholderia pseudomallei	Bp0122	Positive (+)
Burkholderia pseudomallei	Bp0123	Positive (+)
Burkholderia pseudomallei	Bp0127	Positive (+)
Burkholderia pseudomallei	Bp0128	Positive (+)
Burkholderia pseudomallei	Bp0129	Positive (+)
Burkholderia pseudomallei	Bp3539	Positive (+)
Burkholderia pseudomallei	Bp3570	Positive (+)
Burkholderia pseudomallei	Bp3671	Positive (+)
Burkholderia pseudomallei	Bp3994	Positive (+)

Table 2. Continued.

Bacterial isolate	Strain name/DASH #	Lateral flow result
Burkholderia pseudomallei	Bp3999	Positive (+)
Burkholderia pseudomallei	Bp4000	Positive (+)
Burkholderia pseudomallei	Bp4001	Positive (+)
Burkholderia pseudomallei	Bp4003	Positive (+)
Burkholderia pseudomallei	Bp4137	Positive (+)
Burkholderia pseudomallei	Bp4151	Positive (+)
Burkholderia pseudomallei	Bp4154	Positive (+)
Burkholderia pseudomallei	Bp4160	Positive (+)
Burkholderia pseudomallei	Bp4162	Positive (+)
Burkholderia pseudomallei	Bp4164	Positive (+)
Burkholderia pseudomallei	Bp4169	Positive (+)
Burkholderia mallei	AGD0001147	Positive (+)
Burkholderia mallei	AGD0001235	Positive (+)
Burkholderia mallei	AGD0000503	Positive (+)

References

1. **Limmathurotsakul D, Wongratanacheewin S, Teerawattanasook N, Wongsuvan G, Chaisuksant S, Chetchotisakd P, Chaowagul W, Day NP, Peacock SJ.** 2010. Increasing incidence of human melioidosis in Northeast Thailand. Am. J. Trop. Med. Hyg. **82:**1113-1117.

2. **Currie BJ, Fisher DA, Howard DM, Burrow JN, Lo D, Selva-Nayagam S, Anstey NM, Huffam SE, Snelling PL, Marks PJ, Stephens DP, Lum GD, Jacups SP, Krause VL.** 2000. Endemic melioidosis in tropical northern Australia: a 10-year prospective study and review of the literature. Clin. Infect. Dis. **31:**981-986.

3. **Chaowagul W, Suputtamongkol Y, Dance DA, Rajchanuvong A, Pattara-arechachai J, White NJ.** 1993. Relapse in melioidosis: incidence and risk factors. J. Infect. Dis. **168:**1181-1185.

4. **Sarkar-Tyson M, Titball RW.** 2010. Progress toward development of vaccines against melioidosis: A review. Clin. Ther. **32:**1437-1445.

5. **Currie BJ, Ward L, Cheng AC.** 2010. The epidemiology and clinical spectrum of melioidosis: 540 cases from the 20 year Darwin prospective study. PLoS Negl. Trop. Dis. **4:**e900.

6. **Mays EE, Ricketts EA.** 1975. Melioidosis: recrudescence associated with bronchogenic carcinoma twenty-six years following initial geographic exposure. Chest **68:**261-263.

7. **Ngauy V, Lemeshev Y, Sadkowski L, Crawford G.** 2005. Cutaneous melioidosis in a man who was taken as a prisoner of war by the Japanese during World War II. J. Clin. Microbiol. **43:**970-972.

8. **Wuthiekanun V, Amornchai P, Saiprom N, Chantratita N, Chierakul W, Koh GC, Chaowagul W, Day NP, Limmathurotsakul D, Peacock SJ.** 2011. Survey of antimicrobial resistance in clinical Burkholderia pseudomallei isolates over two decades in Northeast Thailand. Antimicrob. Agents Chemother. **55:**5388-5391.

9. **Limmathurotsakul D, Jamsen K, Arayawichanont A, Simpson JA, White LJ, Lee SJ, Wuthiekanun V, Chantratita N, Cheng A, Day NP, Verzilli C, Peacock SJ.** 2010. Defining the true sensitivity of culture for the diagnosis of melioidosis using Bayesian latent class models. PLoS One **5:**e12485.

10. **Heiss C, Burtnick MN, Wang Z, Azadi P, Brett PJ.** 2012. Structural analysis of capsular polysaccharides expressed by Burkholderia mallei and Burkholderia pseudomallei. Carbohydr. Res. **349:**90-94.

11. **Reckseidler-Zenteno SL, DeVinney R, Woods DE.** 2005. The capsular polysaccharide of Burkholderia pseudomallei contributes to survival in serum by reducing complement factor C3b deposition. Infect. Immun. **73:**1106-1115.

12. **Reckseidler SL, DeShazer D, Sokol PA, Woods DE.** 2001. Detection of bacterial virulence genes by subtractive hybridization: identification of

capsular polysaccharide of Burkholderia pseudomallei as a major virulence determinant. Infect. Immun. **69:**34-44.

13. **Cheng AC, Currie BJ.** 2005. Melioidosis: epidemiology, pathophysiology, and management. Clin. Microbiol. Rev. **18:**383-416.

14. **Wilkinson JF.** 1958. The extracellular polysaccharides of bacteria. Bacteriol Rev. **22:**46-73.

15. **Feldmann M, Easten A.** 1971. The relationship between antigenic structure and the requirement for thymus-derived cells in the immune response. J. Exp. Med. **134:**103-119.

16. **Vos Q, Lees A, Wu ZQ, Snapper CM, Mond JJ.** 2000. B-cell activation by T-cell-independent type 2 antigens as an integral part of the humoral immune response to pathogenic microorganisms. Immunol. Rev. **176:**154-170.

17. **Nuti DE, Crump RB, Dwi Handayani F, Chantratita N, Peacock SJ, Bowen R, Felgner PL, Davies DH, Wu T, Lyons CR, Brett PJ, Burtnick MN, Kozel TR, AuCoin DP.** 2011. Identification of circulating bacterial antigens by in vivo microbial antigen discovery. MBio **2**.

18. **Houghton RL, Reed DE, Hubbard MA, Dillon MJ, Chen H, Currie BJ, Mayo M, Sarovich DS, Theobald V, Limmathurotsakul D, Wongsuvan G, Chantratita N, Peacock SJ, Hoffmaster AR, Duval B, Brett PJ, Burtnick MN, Aucoin DP.** 2014. Development of a prototype lateral flow

immunoassay (LFI) for the rapid diagnosis of melioidosis. PLoS Negl. Trop. Dis. **8:**e2727.

19. **Perlmutter RM, Hansburg D, Briles DE, Nicolotti RA, Davie JM.** 1978. Subclass restriction of murine anti-carbohydrate antibodies. J. Immunol. **121:**566-572.

20. **Hansburg D, Perlmutter RM, Briles DE, Davie JM.** 1978. Analysis of the diversity of murine antibodies to dextran B1355. III. Idiotypic and spectrotypic correlations. Eur. J. Immunol. **8:**352-359.

21. **Slack J, Der-Balian GP, Nahm M, Davie JM.** 1980. Subclass restriction of murine antibodies. II. The IgG plaque-forming cell response to thymus-independent type 1 and type 2 antigens in normal mice and mice expressing an X-linked immunodeficiency. J. Exp. Med. **151:**853-862.

22. **Greenspan NS, Dacek DA, Cooper LJ.** 1989. Cooperative binding of two antibodies to independent antigens by an Fc-dependent mechanism. FASEB J. **3:**2203-2207.

23. **Cooper LJ, Schimenti JC, Glass DD, Greenspan NS.** 1991. H chain C domains influence the strength of binding of IgG for streptococcal group A carbohydrate. J. Immunol. **146:**2659-2663.

24. **Cooper LJ, Robertson D, Granzow R, Greenspan NS.** 1994. Variable domain-identical antibodies exhibit IgG subclass-related differences in affinity and kinetic constants as determined by surface plasmon resonance. Mol. Immunol. **31:**577-584.

25. **AuCoin DP, Reed DE, Marlenee NL, Bowen RA, Thorkildson P, Judy BM, Torres AG, Kozel TR.** 2012. Polysaccharide specific monoclonal antibodies provide passive protection against intranasal challenge with Burkholderia pseudomallei. PLoS One **7:**e35386.

26. **Burtnick MN, Heiss C, Roberts RA, Schweizer HP, Azadi P, Brett PJ.** 2012. Development of capsular polysaccharide-based glycoconjugates for immunization against melioidosis and glanders. Front Cell Infect Microbiol **2:**108.

27. **Kozel TR, Murphy WJ, Brandt S, Blazar BR, Lovchik JA, Thorkildson P, Percival A, Lyons CR.** 2004. mAbs to Bacillus anthracis capsular antigen for immunoprotection in anthrax and detection of antigenemia. Proc. Natl. Acad. Sci. U. S. A. **101:**5042-5047.

28. **Hovenden M, Hubbard MA, Aucoin DP, Thorkildson P, Reed DE, Welch WH, Lyons CR, Lovchik JA, Kozel TR.** 2013. IgG subclass and heavy chain domains contribute to binding and protection by mAbs to the poly γ-D-glutamic acid capsular antigen of Bacillus anthracis. PLoS Pathog. **9:**e1003306.

29. **Kozel TR, Hermerath CA.** 1988. Benzoquinone activation of Cryptococcus neoformans capsular polysaccharide for construction of an immunoaffinity column. J. Immunol. Methods **107:**53-58.

30. **DeShazer D, Waag DM, Fritz DL, Woods DE.** 2001. Identification of a Burkholderia mallei polysaccharide gene cluster by subtractive

hybridization and demonstration that the encoded capsule is an essential virulence determinant. Microb. Pathog. **30:**253-269.

31. **Mahenthiralingam E, Urban TA, Goldberg JB.** 2005. The multifarious, multireplicon Burkholderia cepacia complex. Nat Rev Microbiol **3:**144-156.

32. **Bartlett JG.** 2011. Diagnostic tests for agents of community-acquired pneumonia. Clin. Infect. Dis. **52 Suppl 4:**S296-304.

33. **Posthuma-Trumpie GA, Korf J, van Amerongen A.** 2009. Lateral flow (immuno)assay: its strengths, weaknesses, opportunities and threats. A literature survey. Anal Bioanal Chem **393:**569-582.

34. **Tandhavanant S, Wongsuvan G, Wuthiekanun V, Teerawattanasook N, Day NP, Limmathurotsakul D, Peacock SJ, Chantratita N.** 2013. Monoclonal antibody-based immunofluorescence microscopy for the rapid identification of Burkholderia pseudomallei in clinical specimens. Am. J. Trop. Med. Hyg. **89:**165-168.

35. **Rattanathongkom A, Sermswan RW, Wongratanacheewin S.** 1997. Detection of Burkholderia pseudomallei in blood samples using polymerase chain reaction. Mol. Cell. Probes **11:**25-31.

36. **Khupulsup K, Petchclai B.** 1986. Application of indirect hemagglutination test and indirect fluorescent antibody test for IgM antibody for diagnosis of melioidosis in Thailand. Am. J. Trop. Med. Hyg. **35:**366-369.

37. **Cheng AC, Peacock SJ, Limmathurotsakul D, Wongsuvan G, Chierakul W, Amornchai P, Getchalarat N, Chaowagul W, White NJ,**

Day NP, Wuthiekanun V. 2006. Prospective evaluation of a rapid immunochromogenic cassette test for the diagnosis of melioidosis in northeast Thailand. Trans. R. Soc. Trop. Med. Hyg. **100:**64-67.

38. **Kanaphun P, Thirawattanasuk N, Suputtamongkol Y, Naigowit P, Dance DA, Smith MD, White NJ.** 1993. Serology and carriage of Pseudomonas pseudomallei: a prospective study in 1000 hospitalized children in northeast Thailand. J. Infect. Dis. **167:**230-233.

39. **Cuccui J, Milne TS, Harmer N, George AJ, Harding SV, Dean RE, Scott AE, Sarkar-Tyson M, Wren BW, Titball RW, Prior JL.** 2012. Characterization of the Burkholderia pseudomallei K96243 capsular polysaccharide I coding region. Infect. Immun. **80:**1209-1221.

40. **Propst KL, Mima T, Choi KH, Dow SW, Schweizer HP.** 2010. A Burkholderia pseudomallei deltapurM mutant is avirulent in immunocompetent and immunodeficient animals: candidate strain for exclusion from select-agent lists. Infect. Immun. **78:**3136-3143.

41. **Collins AM, Jackson KJ.** 2013. A Temporal Model of Human IgE and IgG Antibody Function. Front. Immunol. **4:**235.

Discussion

Capsules are important virulence factors that are produced by many pathogenic microbes, including *B. pseudomallei and B. mallei*. Capsules are antiphagocytic and prevent complement deposition on the surface of the bacterium (39, 47). Antibodies that target the capsule enhance phagocytosis and complement deposition, making them a critical part of any host defense against an encapsulated pathogen (47). There are several examples where patient survival rates correlate with high antibody titers against capsules (1, 84-86). Capsules are high molecular weight antigens that are comprised of several repeating epitopes. As such, they are T cell-independent type-2 antigens, are poorly immunogenic, and do not elicit a robust humoral immune response. Additionally, capsules are structurally diverse and unique to each organism; immunity to one capsule type does not confer immunity to other capsule types. Despite their incredible importance, there are relatively few studies to explain the molecular interactions between antibodies and capsules. The goal of the present study was to develop a library of monoclonal antibodies, including two full IgG subclass families, targeting the *B. pseudomallei* capsule in order to elucidate *in vitro* correlates of protective antibodies. Additionally, these antibodies have been incorporated into an Active Melioidosis Detect™ Lateral Flow Immunoassay (AMD LFI) in order to rapidly detect *B. pseudomallei* infection in endemic areas.

Antibodies have been used to treat disease since the late 1800's when Kitasato Shibasaburo and Emil von Behring showed that the serum from

immunized guinea pigs could be used treat human diphtheria (87). Serum therapy became very popular, with a treatment for tetanus being developed shortly thereafter (87). More recently serum therapy has been used to treat Ebola hemorrhagic fever (76).

Two important characteristics of anti-capsular protective antibodies are i) high affinity and ii) a rim-type quellung reaction (36, 88-91). Affinity establishes how strongly an antibody binds its antigenic target; a high affinity antibody is more likely to remain bound to its target so it can perform effector functions, like complement activation or antibody-mediated opsonization. A quellung reaction is used to visualize how an antibody binds to a microbial capsule by differential interference contrast (DIC) microscopy (92). Antibodies can cross-link around the perimeter of the capsule, enclosing it in a tight rim or shell. Alternatively, they can bind throughout the capsule, leaving it open and puffy (93).

Rim-type patterns by microscopy correlate with antibody opsonization of the pathogenic yeast, *Cryptococcus neoformans* (94). This could be because it is easier for phagocytes to interact with antibodies binding at the capsular edge versus throughout the capsule. The *C. neoformans* capsule is very large and very fluid, making it difficult for phagocytes to interact with bound antibody F_C receptors (94). Increasing phagocyte receptor mobility increases opsonization (95-97). The inverse may also be true; reducing capsule mobility may also increase opsonization.

High affinity, rim-type antibodies to the capsule of *B. anthracis* are protective (89). Subclass-switching a protective IgG_3 to any other subclass (IgG_1, IgG_{2b}, IgG_{2a}) results in an antibody that is low affinity and forms a puffy-type quellung reaction (98). As expected, the subclass-switch antibodies are non-protective in a murine model of pulmonary anthrax. Additionally, when converting this same IgG_3 mAb into human chimeric antibodies (chAbs), the resulting chAbs have greatly reduced affinity and produce a puffy-type quellung reaction (99).

Subclass-switching the protective, anti-CPS IgG_3 mAb, 3C5, yields similar results (Chapter 1). The IgG_3 subclass is high affinity and is protective in a murine model of pulmonary melioidosis (median time-to-death (MDT) of 31 days) (36); the subclass-switch antibodies are low affinity, react poorly with CPS via ELISA, and provide significantly less protection (MTD of 4 days). Removal of the IgG_3 F_C region by proteolytic cleavage generates low affinity $F(ab')_2$ fragments that react with CPS poorly via ELISA. Subclass-switch antibodies are antibodies that have identical F_V regions but different heavy chain constant regions. Thus, they bind to the exact same epitope, but have different effector functions. This suggests that something in the constant region is contributing to the drop in affinity and lack of protection. The constant region itself is not solely responsible for the IgG_3's high affinity; we have generated several high affinity IgG_1 mAbs that react strongly with CPS on ELISA and are protective in a murine model of pulmonary melioidosis (Chapter 1). Subclass-switching a high affinity IgG_1 mAb,

2A5, yields high affinity IgG_{2b} and IgG_{2a} antibodies with no significant drop in animal protection.

One hypothesis for this is that our IgG_3 mAb, 3C5, only has a high affinity because of the cooperative binding phenomena seen in IgG_3 mAbs. The F_C regions cross-link; cross-linking assists the antibodies in both binding to their target and remaining bound by keeping them in proximity to the antigen (100). Altering or removal of the IgG_3 F_C region eliminates cooperative binding and the affinity increase that it provides. This idea is supported by the fact that protective antibodies do not have to be of the IgG_3 subclass. IgG_1, IgG_{2b}, and IgG_{2a} variants of mAb 2A5 were all significantly protective in a murine model of pulmonary melioidosis (Chapter 1). Additionally, IgG_1 mAbs targeting the capsule of *C. neoformans* can be generated with high affinity, can form a rim-type pattern, and be protective in a murine model of *C. neoformans* infection (88, 101, 102). Unfortunately, *B. pseudomallei* is too small to be visualized with DIC microscopy (2-5 *μ*m length, 0.4-0.8 *μ*m diameter). Thus, a quellung reaction could not be observed; however, we believe the IgG_3 variant of mAb 3C5 may form a rim-type pattern and the subclass-switch mAbs may form a puffy-type pattern. Furthermore, we hypothesize that all of the 2A5 variants would form rim-type patterns. Taken together, these results indicate that protection is subclass-independent. High affinity mAbs of all subclasses have been shown to be protective in a murine model of melioidosis. Thus, immunization strategies should prioritize generating a high affinity antibody response.

Another goal of the present study was to generate a library of high affinity anti-CPS antibodies of different IgG subclasses for the diagnosis of melioidosis. Melioidosis is rampant in developing and resource poor nations in Southeast Asia and claims an estimated 250,000 lives each year (personal communication from Dr. Direk Limmathurotsakul). This is partially due to how difficult melioidosis is to diagnose; *B. pseudomallei* has been called "the great mimicker" patients present with symptoms similar to many other common infections (103). Rapid diagnosis of melioidosis is critical. Delays in treatment are associated with higher rates patient relapse and mortality (1). However, there has been limited success developing diagnostic methods that are both rapid and accessible to resource poor countries. Current methods are time consuming, expensive to implement, and inaccurate (10). As such, we previously developed a prototype Active Melioidosis Detect™ Lateral Flow Immunoassay using IgG$_3$ mAb 3C5 (104). The AMD LFI was highly successful; it could detect CPS in patient samples and identify *B. pseudomallei* colonies picked from agar plates. Tests were inexpensive to produce and could be performed in 10 minutes.

Unfortunately, there were some background issues believed to be occurring due to IgG$_3$-IgG$_3$ interactions. LFI assays are analogous to ELISA sandwich assays; an immobilized antibody binds to one side of the antigen while a second, labeled, antibody binds to the other side. Without addition of antigen, there should be no ELISA signal, however, the cross-linking ability of IgG$_3$ mAbs appears to be causing high background signals with negative control samples.

Thus, one of the goals of the present study was to reduce the background signal of the AMD LFI.

As previously mentioned, capsules are weakly immunogenic and do not elicit a strong humoral immune response. IgG_3 is the predominant subclass in response to a polysaccharide antigen in mice (105-107). Therefore, we immunized mice with CPS-BSA glycoconjugate (27). Glycoconjugate vaccines are available for a wide variety of pathogens, including *Haemophilus influenzae*, *Neisseria meningitidis*, and *Streptococcus pneumoniae*. They conjugate the weakly immunogenic capsular structure with a highly immunogenic protein or toxoid in order to generate a strong humoral immune response and elicit immunological memory. The CPS-BSA glycoconjugate was highly effective; we were able to generate seven IgG_1 mAbs that target the CPS of *B. pseudomallei*.

Of the seven antibodies generated, one has a 3-fold lower affinity than mAb 3C5 (mAb 3B4), two have similar affinities to mAb 3C5 (mAb 1A2 and mAb 2A5) and one has a five-fold greater affinity (mAb 4C4). Additionally, mAbs 3B4, 1A2, and 2A5 all react similarly to mAb 3C5 in direct binding ELISA while mAb 4C4 performed best. The three remaining mAbs had affinities that were too low to accurately assess. Additionally, they performed very poorly in direct antigen ELISAs. Of the low affinity antibodies two were IgM (mAb 2B3 and mAb 1D4) and one was an IgG_1 (mAb 1D3). This was not wholly unexpected. IgM antibodies are typically rapidly generated, low-affinity first responders that have not had the opportunity to affinity mature (65). They can overcome their intrinsic weak low-

affinity by forming polymers of pentamers and hexamers; however, we hypothesize that as with IgG_3 mAbs, the polymeric nature of IgM mAbs would be detrimental to the AMD LFI, thus, we did not pursue additional studies with these mAbs.

In order to determine which mAbs might function best on an LFI, we tested our library via sandwich ELISA. Our hypothesis was that a higher affinity antibody would be able to detect smaller amounts of CPS in patient samples. Results were mixed. As expected, mAb 4C4 (5-fold greater affinity than 3C5) could detect smaller concentrations of CPS in samples. However, we noticed no pattern among the remaining mAbs. For example, mAb 2A5 (similar affinity to 3C5) performed four-fold worse while mAb 3B4 (3-fold lower affinity than 3C5) only performed 2-fold worse. Results were similar when we used the library to create LFIs. These results indicate that affinity does not directly correlate with LFI performance.

In summary, we have characterized a library of 15 mAbs, including 2 subclass families, targeting the CPS of *B. pseudomallei* and determined some ideal characteristics for mAbs used in therapeutics and diagnostics. IgG_3 is the default response to polysaccharide antigens in mice; however, therapeutic mAbs can be of any IgG subclass, as long as they have a high affinity. These results are in agreement with studies involving both *B. anthracis* and *C. neoformans*. Both IgG_3 and non-IgG_3 mAbs can be protective in a murine model of pulmonary anthrax and the higher affinity antibodies are more protective (89, 90).

Furthermore, IgG$_1$ mAbs provide the highest rates of protection in a murine model of cryptococcal meningitis (101, 108).

Be that as it may, IgG$_3$ mAbs are not the best candidates for use in LFIs as they tend to self-aggregate and produce false positive results. IgG$_1$ mAbs seem to work well; however, when there are multiple candidates, it is difficult to predict which mAb will function best based on affinity or ELISA alone. The mAbs must be tested in the format they will be used in.

References

1. **Cheng AC, Currie BJ.** 2005. Melioidosis: epidemiology, pathophysiology, and management. Clin. Microbiol. Rev. **18:**383-416.

2. **Kanaphun P, Thirawattanasuk N, Suputtamongkol Y, Naigowit P, Dance DA, Smith MD, White NJ.** 1993. Serology and carriage of Pseudomonas pseudomallei: a prospective study in 1000 hospitalized children in northeast Thailand. J. Infect. Dis. **167:**230-233.

3. **Wiersinga WJ, Currie BJ, Peacock SJ.** 2012. Melioidosis. N. Engl. J. Med. **367:**1035-1044.

4. **Koh GC, Maude RR, Schreiber MF, Limmathurotsakul D, Wiersinga WJ, Wuthiekanun V, Lee SJ, Mahavanakul W, Chaowagul W, Chierakul W, White NJ, van der Poll T, Day NP, Dougan G, Peacock SJ.** 2011. Glyburide is anti-inflammatory and associated with reduced mortality in melioidosis. Clin. Infect. Dis. **52:**717-725.

5. **Alba-Loureiro TC, Munhoz CD, Martins JO, Cerchiaro GA, Scavone C, Curi R, Sannomiya P.** 2007. Neutrophil function and metabolism in individuals with diabetes mellitus. Braz. J. Med. Biol. Res. **40:**1037-1044.

6. **Limmathurotsakul D, Wongratanacheewin S, Teerawattanasook N, Wongsuvan G, Chaisuksant S, Chetchotisakd P, Chaowagul W, Day NP, Peacock SJ.** 2010. Increasing incidence of human melioidosis in Northeast Thailand. Am. J. Trop. Med. Hyg. **82:**1113-1117.

7. **Currie BJ, Ward L, Cheng AC.** 2010. The epidemiology and clinical spectrum of melioidosis: 540 cases from the 20 year Darwin prospective study. PLoS Negl. Trop. Dis. **4:**e900.

8. **Mays EE, Ricketts EA.** 1975. Melioidosis: recrudescence associated with bronchogenic carcinoma twenty-six years following initial geographic exposure. Chest **68:**261-263.

9. **Ngauy V, Lemeshev Y, Sadkowski L, Crawford G.** 2005. Cutaneous melioidosis in a man who was taken as a prisoner of war by the Japanese during World War II. J. Clin. Microbiol. **43:**970-972.

10. **Limmathurotsakul D, Jamsen K, Arayawichanont A, Simpson JA, White LJ, Lee SJ, Wuthiekanun V, Chantratita N, Cheng A, Day NP, Verzilli C, Peacock SJ.** 2010. Defining the true sensitivity of culture for the diagnosis of melioidosis using Bayesian latent class models. PLoS One **5:**e12485.

11. **Rattanathongkom A, Sermswan RW, Wongratanacheewin S.** 1997. Detection of Burkholderia pseudomallei in blood samples using polymerase chain reaction. Mol. Cell. Probes **11:**25-31.

12. **Khupulsup K, Petchclai B.** 1986. Application of indirect hemagglutination test and indirect fluorescent antibody test for IgM antibody for diagnosis of melioidosis in Thailand. Am. J. Trop. Med. Hyg. **35:**366-369.

13. **Cheng AC, Peacock SJ, Limmathurotsakul D, Wongsuvan G, Chierakul W, Amornchai P, Getchalarat N, Chaowagul W, White NJ,**

Day NP, Wuthiekanun V. 2006. Prospective evaluation of a rapid immunochromogenic cassette test for the diagnosis of melioidosis in northeast Thailand. Trans. R. Soc. Trop. Med. Hyg. **100:**64-67.

14. **Chantratita N, Wuthiekanun V, Thanwisai A, Limmathurotsakul D, Cheng AC, Chierakul W, Day NP, Peacock SJ.** 2007. Accuracy of enzyme-linked immunosorbent assay using crude and purified antigens for serodiagnosis of melioidosis. Clin. Vaccine Immunol. **14:**110-113.

15. **Tandhavanant S, Wongsuvan G, Wuthiekanun V, Teerawattanasook N, Day NP, Limmathurotsakul D, Peacock SJ, Chantratita N.** 2013. Monoclonal antibody-based immunofluorescence microscopy for the rapid identification of Burkholderia pseudomallei in clinical specimens. Am. J. Trop. Med. Hyg. **89:**165-168.

16. **Meumann EM, Novak RT, Gal D, Kaestli ME, Mayo M, Hanson JP, Spencer E, Glass MB, Gee JE, Wilkins PP, Currie BJ.** 2006. Clinical evaluation of a type III secretion system real-time PCR assay for diagnosing melioidosis. J. Clin. Microbiol. **44:**3028-3030.

17. **Wuthiekanun V, Amornchai P, Saiprom N, Chantratita N, Chierakul W, Koh GC, Chaowagul W, Day NP, Limmathurotsakul D, Peacock SJ.** 2011. Survey of antimicrobial resistance in clinical Burkholderia pseudomallei isolates over two decades in Northeast Thailand. Antimicrob. Agents Chemother. **55:**5388-5391.

18. **Schweizer HP.** 2012. Mechanisms of antibiotic resistance in Burkholderia pseudomallei: implications for treatment of melioidosis. Future Microbiol. **7:**1389-1399.

19. **Chantratita N, Rholl DA, Sim B, Wuthiekanun V, Limmathurotsakul D, Amornchai P, Thanwisai A, Chua HH, Ooi WF, Holden MT, Day NP, Tan P, Schweizer HP, Peacock SJ.** 2011. Antimicrobial resistance to ceftazidime involving loss of penicillin-binding protein 3 in Burkholderia pseudomallei. Proc. Natl. Acad. Sci. U. S. A. **108:**17165-17170.

20. **Cheng AC, McBryde ES, Wuthiekanun V, Chierakul W, Amornchai P, Day NP, White NJ, Peacock SJ.** 2009. Dosing regimens of cotrimoxazole (trimethoprim-sulfamethoxazole) for melioidosis. Antimicrob. Agents Chemother. **53:**4193-4199.

21. **Nelson M, Prior JL, Lever MS, Jones HE, Atkins TP, Titball RW.** 2004. Evaluation of lipopolysaccharide and capsular polysaccharide as subunit vaccines against experimental melioidosis. J. Med. Microbiol. **53:**1177-1182.

22. **Breitbach K, Köhler J, Steinmetz I.** 2008. Induction of protective immunity against Burkholderia pseudomallei using attenuated mutants with defects in the intracellular life cycle. Trans. R. Soc. Trop. Med. Hyg. **102 Suppl 1:**S89-94.

23. **Sarkar-Tyson M, Smither SJ, Harding SV, Atkins TP, Titball RW.** 2009. Protective efficacy of heat-inactivated B. thailandensis, B. mallei or B.

pseudomallei against experimental melioidosis and glanders. Vaccine **27:**4447-4451.

24. **Chen YS, Hsiao YS, Lin HH, Yen CM, Chen SC, Chen YL.** 2006. Immunogenicity and anti-Burkholderia pseudomallei activity in Balb/c mice immunized with plasmid DNA encoding flagellin. Vaccine **24:**750-758.

25. **Nieves W, Asakrah S, Qazi O, Brown KA, Kurtz J, Aucoin DP, McLachlan JB, Roy CJ, Morici LA.** 2011. A naturally derived outer-membrane vesicle vaccine protects against lethal pulmonary Burkholderia pseudomallei infection. Vaccine **29:**8381-8389.

26. **Brett PJ, Woods DE.** 1996. Structural and immunological characterization of Burkholderia pseudomallei O-polysaccharide-flagellin protein conjugates. Infect. Immun. **64:**2824-2828.

27. **Burtnick MN, Heiss C, Roberts RA, Schweizer HP, Azadi P, Brett PJ.** 2012. Development of capsular polysaccharide-based glycoconjugates for immunization against melioidosis and glanders. Front Cell Infect Microbiol **2:**108.

28. **Chaowagul W, Suputtamongkol Y, Dance DA, Rajchanuvong A, Pattara-arechachai J, White NJ.** 1993. Relapse in melioidosis: incidence and risk factors. J. Infect. Dis. **168:**1181-1185.

29. **Currie BJ, Fisher DA, Anstey NM, Jacups SP.** 2000. Melioidosis: acute and chronic disease, relapse and re-activation. Trans. R. Soc. Trop. Med. Hyg. **94:**301-304.

30. **Korbsrisate S, Tomaras AP, Damnin S, Ckumdee J, Srinon V, Lengwehasatit I, Vasil ML, Suparak S.** 2007. Characterization of two distinct phospholipase C enzymes from Burkholderia pseudomallei. Microbiology **153:**1907-1915.

31. **White NJ.** 2003. Melioidosis. Lancet **361:**1715-1722.

32. **Stevens MP, Friebel A, Taylor LA, Wood MW, Brown PJ, Hardt WD, Galyov EE.** 2003. A Burkholderia pseudomallei type III secreted protein, BopE, facilitates bacterial invasion of epithelial cells and exhibits guanine nucleotide exchange factor activity. J. Bacteriol. **185:**4992-4996.

33. **Burtnick MN, Brett PJ, Harding SV, Ngugi SA, Ribot WJ, Chantratita N, Scorpio A, Milne TS, Dean RE, Fritz DL, Peacock SJ, Prior JL, Atkins TP, Deshazer D.** 2011. The cluster 1 type VI secretion system is a major virulence determinant in Burkholderia pseudomallei. Infect. Immun. **79:**1512-1525.

34. **Heiss C, Burtnick MN, Wang Z, Azadi P, Brett PJ.** 2012. Structural analysis of capsular polysaccharides expressed by Burkholderia mallei and Burkholderia pseudomallei. Carbohydr. Res. **349:**90-94.

35. **Reckseidler SL, DeShazer D, Sokol PA, Woods DE.** 2001. Detection of bacterial virulence genes by subtractive hybridization: identification of capsular polysaccharide of Burkholderia pseudomallei as a major virulence determinant. Infect. Immun. **69:**34-44.

36. **AuCoin DP, Reed DE, Marlenee NL, Bowen RA, Thorkildson P, Judy BM, Torres AG, Kozel TR.** 2012. Polysaccharide specific monoclonal antibodies provide passive protection against intranasal challenge with Burkholderia pseudomallei. PLoS One **7:**e35386.

37. **Jones SM, Ellis JF, Russell P, Griffin KF, Oyston PC.** 2002. Passive protection against Burkholderia pseudomallei infection in mice by monoclonal antibodies against capsular polysaccharide, lipopolysaccharide or proteins. J. Med. Microbiol. **51:**1055-1062.

38. **Nuti DE, Crump RB, Dwi Handayani F, Chantratita N, Peacock SJ, Bowen R, Felgner PL, Davies DH, Wu T, Lyons CR, Brett PJ, Burtnick MN, Kozel TR, AuCoin DP.** 2011. Identification of circulating bacterial antigens by in vivo microbial antigen discovery. MBio **2**.

39. **Reckseidler-Zenteno SL, DeVinney R, Woods DE.** 2005. The capsular polysaccharide of Burkholderia pseudomallei contributes to survival in serum by reducing complement factor C3b deposition. Infect. Immun. **73:**1106-1115.

40. **Cuccui J, Milne TS, Harmer N, George AJ, Harding SV, Dean RE, Scott AE, Sarkar-Tyson M, Wren BW, Titball RW, Prior JL.** 2012. Characterization of the Burkholderia pseudomallei K96243 capsular polysaccharide I coding region. Infect. Immun. **80:**1209-1221.

41. **Propst KL, Mima T, Choi KH, Dow SW, Schweizer HP.** 2010. A Burkholderia pseudomallei deltapurM mutant is avirulent in

immunocompetent and immunodeficient animals: candidate strain for exclusion from select-agent lists. Infect. Immun. **78:**3136-3143.

42. **DeVoe IW.** 1982. The meningococcus and mechanisms of pathogenicity. Microbiol. Rev. **46:**162-190.

43. **Yoshida K, Matsumoto T, Tateda K, Uchida K, Tsujimoto S, Yamaguchi K.** 2000. Role of bacterial capsule in local and systemic inflammatory responses of mice during pulmonary infection with Klebsiella pneumoniae. J. Med. Microbiol. **49:**1003-1010.

44. **Crisel RM, Baker RS, Dorman DE.** 1975. Capsular polymer of Haemophilus influenzae, type b. I. Structural characterization of the capsular polymer of strain Eagan. J. Biol. Chem. **250:**4926-4930.

45. **Cherniak R, Valafar H, Morris LC, Valafar F.** 1998. Cryptococcus neoformans chemotyping by quantitative analysis of 1H nuclear magnetic resonance spectra of glucuronoxylomannans with a computer-simulated artificial neural network. Clin. Diagn. Lab. Immunol. **5:**146-159.

46. **Zwartouw HT, Smith H.** 1956. Polyglutamic acid from Bacillus anthracis grown in vivo; structure and aggressin activity. Biochem. J. **63:**437-442.

47. **Wilkinson JF.** 1958. The extracellular polysaccharides of bacteria. Bacteriol Rev. **22:**46-73.

48. **Maxted WR.** 1952. Enhancement of streptococcal bacteriophage lysis by hyaluronidase. Nature **170:**1020-1021.

49. **Vos Q, Lees A, Wu ZQ, Snapper CM, Mond JJ.** 2000. B-cell activation by T-cell-independent type 2 antigens as an integral part of the humoral immune response to pathogenic microorganisms. Immunol. Rev. **176:**154-170.

50. **Hess C, Winkler A, Lorenz AK, Holecska V, Blanchard V, Eiglmeier S, Schoen AL, Bitterling J, Stoehr AD, Petzold D, Schommartz T, Mertes MM, Schoen CT, Tiburzy B, Herrmann A, Köhl J, Manz RA, Madaio MP, Berger M, Wardemann H, Ehlers M.** 2013. T cell-independent B cell activation induces immunosuppressive sialylated IgG antibodies. J. Clin. Invest. **123:**3788-3796.

51. **Dance DA.** 2005. Melioidosis and Glanders as Possible Biological Weapons, p. 99-145. *In* I. W. Fong KA (ed.), Bioterrorism and Infectious Agents: A New Dilemma for the 21st Century. Springer, New York, NY.

52. **Emini EA, Hughes JV, Perlow DS, Boger J.** 1985. Induction of hepatitis A virus-neutralizing antibody by a virus-specific synthetic peptide. J. Virol. **55:**836-839.

53. **Volk WA, Bizzini B, Snyder RM, Bernhard E, Wagner RR.** 1984. Neutralization of tetanus toxin by distinct monoclonal antibodies binding to multiple epitopes on the toxin molecule. Infect. Immun. **45:**604-609.

54. **Cooper NR.** 1985. The classical complement pathway: activation and regulation of the first complement component. Adv. Immunol. **37:**151-216.

55. **Kozel TR, Follette JL.** 1981. Opsonization of encapsulated Cryptococcus neoformans by specific anticapsular antibody. Infect. Immun. **31:**978-984.

56. **Löfgren S, Tärnvik A, Carlsson J.** 1980. Demonstration of opsonizing antibodies to Francisella tularensis by leukocyte chemiluminescence. Infect. Immun. **29:**329-334.

57. **Schellekens GA, de Jong BA, van den Hoogen FH, van de Putte LB, van Venrooij WJ.** 1998. Citrulline is an essential constituent of antigenic determinants recognized by rheumatoid arthritis-specific autoantibodies. J. Clin. Invest. **101:**273-281.

58. **Miller JF, Osoba D.** 1967. Current concepts of the immunological function of the thymus. Physiol. Rev. **47:**437-520.

59. **Feldmann M, Easten A.** 1971. The relationship between antigenic structure and the requirement for thymus-derived cells in the immune response. J. Exp. Med. **134:**103-119.

60. **Tonegawa S, Steinberg C, Dube S, Bernardini A.** 1974. Evidence for somatic generation of antibody diversity. Proc. Natl. Acad. Sci. U. S. A. **71:**4027-4031.

61. **Fanning LJ, Connor AM, Wu GE.** 1996. Development of the immunoglobulin repertoire. Clin. Immunol. Immunopathol. **79:**1-14.

62. **Clark MR.** 1997. IgG effector mechanisms. Chem. Immunol. **65:**88-110.

63. **Corthesy B, Kraehenbuhl JP.** 1999. Antibody-mediated protection of mucosal surfaces. Curr. Top. Microbiol. Immunol. **236:**93-111.

64. **Normansell DE.** 1987. Human immunoglobulin subclasses. Diagn. Clin. Immunol. **5:**115-128.

65. **Collins AM, Jackson KJ.** 2013. A Temporal Model of Human IgE and IgG Antibody Function. Front. Immunol. **4:**235.

66. **Diebolder CA, Beurskens FJ, de Jong RN, Koning RI, Strumane K, Lindorfer MA, Voorhorst M, Ugurlar D, Rosati S, Heck AJ, van de Winkel JG, Wilson IA, Koster AJ, Taylor RP, Saphire EO, Burton DR, Schuurman J, Gros P, Parren PW.** 2014. Complement is activated by IgG hexamers assembled at the cell surface. Science **343:**1260-1263.

67. **Lipman NS, Jackson LR, Trudel LJ, Weis-Garcia F.** 2005. Monoclonal versus polyclonal antibodies: distinguishing characteristics, applications, and information resources. ILAR J **46:**258-268.

68. **Maini R, St Clair EW, Breedveld F, Furst D, Kalden J, Weisman M, Smolen J, Emery P, Harriman G, Feldmann M, Lipsky P.** 1999. Infliximab (chimeric anti-tumour necrosis factor alpha monoclonal antibody) versus placebo in rheumatoid arthritis patients receiving concomitant methotrexate: a randomised phase III trial. ATTRACT Study Group. Lancet **354:**1932-1939.

69. **Robak T.** 2008. Novel monoclonal antibodies for the treatment of chronic lymphocytic leukemia. Curr. Cancer Drug Targets **8:**156-171.

70. **Turner TL, Kopp BT, Paul G, Landgrave LC, Hayes D, Thompson R.** 2014. Respiratory syncytial virus: current and emerging treatment options. Clinicoecon Outcomes Res **6:**217-225.

71. **Köhler G, Milstein C.** 1975. Continuous cultures of fused cells secreting antibody of predefined specificity. Nature **256:**495-497.

72. **Sabin AB.** 1954. Noncytopathogenic variants of poliomyelitis viruses and resistance to superinfection in tissue culture. Science **120:**357.

73. **Salk JE, Krech U, Youngner JS, Bennett BL, Lewis LJ, Bazeley PL.** 1954. Formaldehyde treatment and safety testing of experimental poliomyelitis vaccines. Am. J. Public Health Nations Health **44:**563-570.

74. **Claesson BA, Trollfors B, Lagergard T, Taranger J, Bryla D, Otterman G, Cramton T, Yang Y, Reimer CB, Robbins JB.** 1988. Clinical and immunologic responses to the capsular polysaccharide of Haemophilus influenzae type b alone or conjugated to tetanus toxoid in 18- to 23-month-old children. J. Pediatr. **112:**695-702.

75. **Mankarious S, Lee M, Fischer S, Pyun KH, Ochs HD, Oxelius VA, Wedgwood RJ.** 1988. The half-lives of IgG subclasses and specific antibodies in patients with primary immunodeficiency who are receiving intravenously administered immunoglobulin. J. Lab. Clin. Med. **112:**634-640.

76. **Mupapa K, Massamba M, Kibadi K, Kuvula K, Bwaka A, Kipasa M, Colebunders R, Muyembe-Tamfum JJ.** 1999. Treatment of Ebola

hemorrhagic fever with blood transfusions from convalescent patients. International Scientific and Technical Committee. J. Infect. Dis. **179 Suppl 1:**S18-23.

77. **Tuft L, Ramsdell SG.** 1929. The antibody response in the human being after injection with normal horse serum. J. Exp. Med. **50:**431-437.

78. **Posthuma-Trumpie GA, Korf J, van Amerongen A.** 2009. Lateral flow (immuno)assay: its strengths, weaknesses, opportunities and threats. A literature survey. Anal Bioanal Chem **393:**569-582.

79. **Leuvering JH, Thal PJ, van der Waart M, Schuurs AH.** 1980. Sol particle immunoassay (SPIA). J. Immunoassay **1:**77-91.

80. **van Dam GJ, Wichers JH, Ferreira TM, Ghati D, van Amerongen A, Deelder AM.** 2004. Diagnosis of schistosomiasis by reagent strip test for detection of circulating cathodic antigen. J. Clin. Microbiol. **42:**5458-5461.

81. **Fernández-Sánchez C, McNeil CJ, Rawson K, Nilsson O, Leung HY, Gnanapragasam V.** 2005. One-step immunostrip test for the simultaneous detection of free and total prostate specific antigen in serum. J. Immunol. Methods **307:**1-12.

82. **van Amerongen A, van Loon D, Berendsen LB, Wichers JH.** 1994. Quantitative computer image analysis of a human chorionic gonadotropin colloidal carbon dipstick assay. Clin. Chim. Acta **229:**67-75.

83. **Xia X, Xu Y, Zhao X, Li Q.** 2009. Lateral flow immunoassay using europium chelate-loaded silica nanoparticles as labels. Clin. Chem. **55:**179-182.

84. **Zysk G, Bethe G, Nau R, Koch D, Gräfin Von Bassewitz VC, Heinz HP, Reinert RR.** 2003. Immune response to capsular polysaccharide and surface proteins of Streptococcus pneumoniae in patients with invasive pneumococcal disease. J. Infect. Dis. **187:**330-333.

85. **Goldschneider I, Gotschlich EC, Artenstein MS.** 1969. Human immunity to the meningococcus. I. The role of humoral antibodies. J. Exp. Med. **129:**1307-1326.

86. **Schauer U, Stemberg F, Rieger CH, Büttner W, Borte M, Schubert S, Möllers H, Riedel F, Herz U, Renz H, Herzog W.** 2003. Levels of antibodies specific to tetanus toxoid, Haemophilus influenzae type b, and pneumococcal capsular polysaccharide in healthy children and adults. Clin. Diagn. Lab. Immunol. **10:**202-207.

87. **Von Stabsartzt B.** 1991. Ueber das zustandekommen der diphtherie-immunität und der tetanus-immunität bei thieren. Mol. Immunol. **28:**1319-1320.

88. **Sanford JE, Lupan DM, Schlageter AM, Kozel TR.** 1990. Passive immunization against Cryptococcus neoformans with an isotype-switch family of monoclonal antibodies reactive with cryptococcal polysaccharide. Infect. Immun. **58:**1919-1923.

89.   **Kozel TR, Thorkildson P, Brandt S, Welch WH, Lovchik JA, AuCoin DP, Vilai J, Lyons CR.** 2007. Protective and immunochemical activities of monoclonal antibodies reactive with the Bacillus anthracis polypeptide capsule. Infect. Immun. **75:**152-163.

90.   **Chen Z, Schneerson R, Lovchik J, Lyons CR, Zhao H, Dai Z, Kubler-Kielb J, Leppla SH, Purcell RH.** 2011. Pre- and postexposure protection against virulent anthrax infection in mice by humanized monoclonal antibodies to Bacillus anthracis capsule. Proc. Natl. Acad. Sci. U. S. A. **108:**739-744.

91.   **Kozel TR, Murphy WJ, Brandt S, Blazar BR, Lovchik JA, Thorkildson P, Percival A, Lyons CR.** 2004. mAbs to Bacillus anthracis capsular antigen for immunoprotection in anthrax and detection of antigenemia. Proc. Natl. Acad. Sci. U. S. A. **101:**5042-5047.

92.   **Neufeld F.** 1902. Ueber die Agglutination der Pneumokokken und über die Theorieen der Agglutination. Z. Hyg. Infektionskr. **40:**54-72.

93.   **MacGill TC, MacGill RS, Casadevall A, Kozel TR.** 2000. Biological correlates of capsular (quellung) reactions of Cryptococcus neoformans. J. Immunol. **164:**4835-4842.

94.   **Netski D, Kozel TR.** 2002. Fc-dependent and Fc-independent opsonization of Cryptococcus neoformans by anticapsular monoclonal antibodies: importance of epitope specificity. Infect. Immun. **70:**2812-2819.

95. **Collins HL, Bancroft GJ.** 1992. Cytokine enhancement of complement-dependent phagocytosis by macrophages: synergy of tumor necrosis factor-alpha and granulocyte-macrophage colony-stimulating factor for phagocytosis of Cryptococcus neoformans. Eur. J. Immunol. **22:**1447-1454.

96. **Griffin FM.** 1981. Roles of macrophage Fc and C3b receptors in phagocytosis of immunologically coated Cryptococcus neoformans. Proc. Natl. Acad. Sci. U. S. A. **78:**3853-3857.

97. **Levitz SM, Farrell TP.** 1990. Growth inhibition of Cryptococcus neoformans by cultured human monocytes: role of the capsule, opsonins, the culture surface, and cytokines. Infect. Immun. **58:**1201-1209.

98. **Hovenden M, Hubbard MA, Aucoin DP, Thorkildson P, Reed DE, Welch WH, Lyons CR, Lovchik JA, Kozel TR.** 2013. IgG subclass and heavy chain domains contribute to binding and protection by mAbs to the poly γ-D-glutamic acid capsular antigen of Bacillus anthracis. PLoS Pathog. **9:**e1003306.

99. **Hubbard MA, Thorkildson P, Kozel TR, AuCoin DP.** 2013. Constant domains influence binding of mouse-human chimeric antibodies to the capsular polypeptide of Bacillus anthracis. Virulence **4:**483-488.

100. **Cooper LJ, Schimenti JC, Glass DD, Greenspan NS.** 1991. H chain C domains influence the strength of binding of IgG for streptococcal group A carbohydrate. J. Immunol. **146:**2659-2663.

101. **Mukherjee J, Scharff MD, Casadevall A.** 1992. Protective murine monoclonal antibodies to Cryptococcus neoformans. Infect. Immun. **60:**4534-4541.

102. **Dromer F, Charreire J, Contrepois A, Carbon C, Yeni P.** 1987. Protection of mice against experimental cryptococcosis by anti-Cryptococcus neoformans monoclonal antibody. Infect. Immun. **55:**749-752.

103. **Yee KC, Lee MK, Chua CT, Puthucheary SD.** 1988. Melioidosis, the great mimicker: a report of 10 cases from Malaysia. J. Trop. Med. Hyg. **91:**249-254.

104. **Houghton RL, Reed DE, Hubbard MA, Dillon MJ, Chen H, Currie BJ, Mayo M, Sarovich DS, Theobald V, Limmathurotsakul D, Wongsuvan G, Chantratita N, Peacock SJ, Hoffmaster AR, Duval B, Brett PJ, Burtnick MN, Aucoin DP.** 2014. Development of a prototype lateral flow immunoassay (LFI) for the rapid diagnosis of melioidosis. PLoS Negl. Trop. Dis. **8:**e2727.

105. **Slack J, Der-Balian GP, Nahm M, Davie JM.** 1980. Subclass restriction of murine antibodies. II. The IgG plaque-forming cell response to thymus-independent type 1 and type 2 antigens in normal mice and mice expressing an X-linked immunodeficiency. J. Exp. Med. **151:**853-862.

106. **Hansburg D, Perlmutter RM, Briles DE, Davie JM.** 1978. Analysis of the diversity of murine antibodies to dextran B1355. III. Idiotypic and spectrotypic correlations. Eur. J. Immunol. **8:**352-359.

107. **Perlmutter RM, Hansburg D, Briles DE, Nicolotti RA, Davie JM.** 1978. Subclass restriction of murine anti-carbohydrate antibodies. J. Immunol. **121:**566-572.

108. **Yuan R, Casadevall A, Spira G, Scharff MD.** 1995. Isotype switching from IgG3 to IgG1 converts a nonprotective murine antibody to Cryptococcus neoformans into a protective antibody. J. Immunol. **154:**1810-1816.